



CESPU
INSTITUTO UNIVERSITÁRIO
DE CIÊNCIAS DA SAÚDE

Toxicity of the 3,4- methylenedioxyamphetamine (MDMA) and its enantiomers to *Daphnia magna*, after isolation by semipreparative chromatography

Ana Rita Fernandes Miranda da Costa

Dissertation for the Degree of Master's in Forensic Sciences and Laboratory
Techniques

—

Gandra, November 2022

Ana Rita Fernandes Miranda da Costa

Dissertation for the Degree of Master's in Forensic Sciences and Laboratory
Techniques

**Toxicity of the 3,4-methylenedioxymethamphetamine (MDMA)
and its enantiomers to *Daphnia magna*, after isolation by
semipreparative chromatography**

Work carried out under the guidance of
**Professor Doctor Cláudia Ribeiro, Professor Doctor Maria
Elizabeth Tiritan and Professor Doctor João Soares Carrola**

DECLARATION OF INTEGRITY

I, identified above, declare that I have acted with absolute integrity in the preparation of this Dissertation. I confirm that in all the work leading to its elaboration I did not use any form of falsification of data or the practice of plagiarism (an act by which an individual, even by omission, assumes the authorship of the intellectual work belonging to another, in its entirety or in parts of it). I further declare that all the sentences that I have taken from previous works belonging to other authors have been referenced or written with new words, in which case I have cited the respective bibliographic source.

Acknowledgments

This dissertation was the result of a year of hard work and dedication, which was only possible due to the contribution and support of some persons, to whom I would like to thank:

First, to my family, who made my entire academic journey possible and who were solely responsible for my presence here today. They have been my mainstay throughout these years and have always supported me in my academic choices and in my desire to continue studying. I am referring to my dear mother and stepfather, whose name does not live up to what he really means to me, as he is the person who most contributed to making all this possible.

To my supervisor, Professor Cláudia Ribeiro, a special thanks for all the support, availability, knowledge transmitted, and, above all, for all the tranquillity she transmitted whenever I felt clumsy. Professor Claudia, even if unconsciously, always motivate me and always make me see the positive side of things. At the end of every meeting we had, I always left with a feeling of relief and that things were going to work out. I'm sure I couldn't have had a better mentor. Thank you so much for your dedication to your amazing work and for the exceptional person you are.

To the co-supervisors, Professor Maria Elizabeth Tiritan and Professor João Soares Carrola, for your availability, help and shared knowledge. Each one had its value that, together, complemented each other. Professor Elizabeth for her in-depth knowledge of chiral chromatography. And Professor João for his experience in toxicity tests on aquatic organisms.

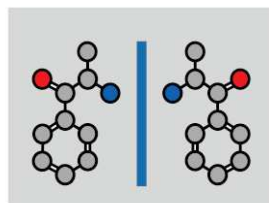
I also thank Professor Bruno Castro for his help in the statistical treatment of the data, to make the study as reliable as possible. I also thank to Virgínia Gonçalves for all her support during separation of the enantiomers and Professor Nuno, for his contribution during the crystallization process and to my colleagues with whom I shared the laboratory, Ariana, Rita, Ivan and Maria, for their contribution to this study and for sharing knowledge, to which I am very grateful.

To all the professors with whom I had the privilege of contacting throughout my journey at the University Institute of Health Sciences, I express my sincere gratitude for all the

experiences, opinions and knowledge transmitted. Undoubtedly, they all contributed to my professional and personal growth.

Finally, to the Toxicology Research Unit (TOXRUN) of the University Institute of Health Sciences, for all the support in terms of equipment and facilities for the execution of this work.

This work was funded by national funds through FCT/MCTES (PIDDAC), under the PTDC/CTA-AMB/6686/2020 project. This research was also partially supported by Strategic Funding UIDB/04423/2021 and UIDP/04423/2021, through national funds provided by the FCT- (ERDF).



EnantioTox



Part of the results presented in this dissertation were used in the following scientific

communication:

Poster communication:

Costa, A., Pérez-Pereira, A., Carvalho, A., Castro, B., Carrola, J., Tiritan, M., & Ribeiro, C. (2022). MDMA effects on *Daphnia magna* morphophysiology: preliminary data. APCF-TOXRUN International Congress 2022, 7-8 April 2022, Gandra, Portugal. (Abstract and poster communication in annex I).

Abstract in index journals:

Costa, A., Pérez-Pereira, A., Carvalho, A., Castro, B., Carrola, J., Tiritan, M., & Ribeiro, C. (2022). MDMA effects on *Daphnia magna* morphophysiology: preliminary data. *RevSALUS - Revista Científica Internacional Da Rede Académica Das Ciências Da Saúde Da Lusofonia*, 4(Sup), 110–111. <https://doi.org/10.51126/revsalus.v4iSup.338>;

Articles in international peer-reviewed journals:

Costa, A., Gonçalves, V., Castro, B.B., Carrola, J.S., Langa, I., Pereira, A., Carvalho, A.R., Tiritan, M.E., Ribeiro, C. (2022). Toxicity of the 3,4-methylenedioxymethamphetamine (MDMA) and its enantiomers to *Daphnia magna*, after isolation by semipreparative chromatography. (in preparation to be submitted to *Molecules*).

Abstract

Psychoactive substances (PAS) have been frequently documented in aquatic systems causing concern for their potential to interfere with biochemical, cellular, physiological, and behavioural mechanisms of non-target organisms. 3,4-Methylenedioxymethamphetamine (MDMA) is among the most consumed PAS in the world. However, the United States Food and Drugs Administration (USFDA) recently approved a trial to assess its pharmacological potential in patients with post-traumatic stress disorder.

MDMA is a chiral substance, sold on the illicit market exclusively as a racemate (*R,S*-MDMA). After consumption, human metabolism is enantioselective, *S*(+)-MDMA undergo preferential metabolism over *R*(-)-MDMA, which leads to enrichment of the *R*(-)-enantiomer in excretions. Its occurrence in the environment arises from direct disposal of sewage, clandestine laboratories or discharges of effluents from Wastewater Treatment Plants (WWTPs) due to the inefficiency of WWTP to completely eliminate drugs residues.

Studies on the toxicity of this compound in non-target organisms are scarce and lack of information on enantioselectivity. Thus, the objective of this work was to evaluate the enantioselective potential on MDMA toxicity using *Daphnia magna* as a freshwater animal model. For this, the MDMA enantiomers were separated by semi-preparative chromatography using a semi-preparative column with amylose tris-3,5-dimethylphenylcarbamate adsorbed on aminopropyl silica (APS-Nucleosil - 500 Å, 7 µm; 20% g/ g). Enantiomers were obtained with an enantiomeric purity > 97% and used in ecotoxicity assay. The sub-chronic assay was initiated with neonates (< 24 h, day 0) through day 8, using three concentrations for the racemate, 0.1, 1.0 and 10.0 µg/L, two concentrations for the enantiomers (0.1 and 1.0 µg/L) and a control group. Each experimental unit consisted of a group of 15 organisms and 5 replicates for each concentration or control and morphophysiological, behavioural, reproductive and biochemical parameters were determined at different stages of the organism's development.

Changes were observed for some of the analyzed parameters as well as enantioselectivity. For example, an increase in body size was observed in organisms exposed to (*R,S*)-MDMA at day 8 (adults) and an enantioselective effect with significantly reduced body growth in organisms exposed to the *S*(+)-enantiomer also at day 8 (adults). Changes in

swimming behaviour were observed with increasing swimming speed and total distance travelled in organisms exposed to (*R,S*)-MDMA at all concentrations. On the contrary, a decrease in the total distance travelled was observed in organisms exposed to the enantiomers but enantioselective effects were not observed. No reproductive or biochemical changes were observed in either racemate or enantiomer exposure except for acetylcholinesterase and catalase activity, whose activity decreased in organisms exposed to the highest concentration of (*R,S*)-MDMA (10 µg/L). This study demonstrated that MDMA can affect the development and swimming behaviour of daphnia including at environmental concentrations and that these effects may be enantioselective, but no reproductive and biochemical changes were observed for the majority of the parameters analysed. However, it is essential to carry out additional studies to complement the results obtained, for an accurate assessment of the potential environmental risks of this substance.

Keywords: *Daphnia magna*; Chirality; Ecotoxicity; Enantioselectivity; Enantioseparation; MDMA.

Resumo

A presença de substâncias psicoativas (SPA) tem sido frequentemente documentada nos ecossistemas aquáticos devido ao seu potencial de interferir com os mecanismos bioquímicos, celulares fisiológicos e comportamentais de organismos não-alvo. A 3,4-metilenodioximetanfetamina (MDMA) encontra-se entre as SPA ilícitas mais consumidas no mundo. No entanto, a United States *Food and Drug Administration* (USFDA), aprovou recentemente um ensaio para a avaliação do seu potencial terapêutico em pacientes com transtorno de stress pós-traumático.

A MDMA é uma substância quirál, vendida no mercado ilícito exclusivamente como racemato (*R,S*)-MDMA. Após consumo, o metabolismo humano é enantiosseletivo, o *S*(+)-MDMA sofre metabolismo preferencial sobre o *R*(-)-MDMA, o que leva ao enriquecimento do enantiomero *R*(-) nas excreções. A sua ocorrência no ambiente surge por descarte direto de esgotos, laboratórios clandestinos ou descargas de efluentes das Estações de tratamento de Águas Residuais (ETAR) devido à ineficiência das ETAR em eliminar totalmente os resíduos de drogas.

Os estudos sobre a toxicidade deste composto em organismos não alvo são escassos e, carecem de informação sobre a enantiosseletividade. Desta forma, o objetivo principal deste trabalho foi avaliar o potencial enantiosseletivo na toxicidade da MDMA usando a *Daphnia magna* como modelo animal de água doce. Para tal, os enantiómeros da MDMA foram separados por cromatografia semi-preparativa utilizando a coluna semi-preparativa *tris*- 3,5 dimetilfenilcarbamato de amilose adsorvido em aminopropil sílica (APS-Nucleosil - 500 Å, 7 µm; 20% g/g). Os enantiómeros foram obtidos com um grau de pureza enantiomérica > 97% e utilizados no ensaio de ecotoxicidade. O ensaio sub-crónico foi iniciado com neonatos (< 24 h, dia 0) até ao dia 8, utilizando três concentrações para o racemato, 0,1, 1,0 e 10,0 µg/L, duas concentrações para os enantiómeros (0,1 e 1,0 µg/L) e um grupo controlo. Cada unidade experimental consistiu num grupo de 15 organismos e 5 réplicas por cada concentração ou controlo e foram determinados parâmetros morfofisiológicos, comportamentais, reprodutivos e bioquímicos em diferentes fases do desenvolvimento do organismo.

Foram observadas alterações para alguns dos parâmetros analisados assim como enantiosseletividade. Por exemplo, foi observado um aumento do tamanho do corpo nos organismos expostos ao (*R,S*)-MDMA no dia 8 (adultos) e um efeito enantiosseletivo com redução significativa do crescimento do corpo nos organismos expostos ao

enantiómero *S*(+) também ao dia 8 (adultos). Foram observadas alterações no comportamento natatório com o aumento da velocidade e distância total percorrida nos organismos expostos ao racemato em todas as concentrações. Pelo contrário, foi observado um decréscimo da distância total percorrida nos organismos expostos aos enantiómeros mas não foram observados efeitos enantiosseletivos. Não foram observadas alterações reprodutivas ou bioquímicas quer na exposição ao racemato quer aos enantiómeros exceto na atividade da acetilcolinesterase e da catalase cuja atividade diminuiu nos organismos expostos à concentração mais elevada do (*R,S*)-MDMA (10 µg/L). Este estudo demonstrou que a MDMA pode afetar o desenvolvimento e o comportamento natatório da dáfnia inclusive para concentrações ambientalmente relevantes e que esses efeitos podem ser enantiosseletivos, mas não foram observadas alterações reprodutivas e bioquímicas para a maioria dos parâmetros analisados. No entanto, é essencial a realização de estudos adicionais para complementar os resultados obtidos, para uma avaliação precisa dos potenciais riscos ambientais desta substância.

Palavras-chave: *Daphnia magna*; Quiralidade; Ecotoxicidade; Enantioseletividade; Enantioseparação; MDMA.

Index

Abstract.....	i
Resumo	iii
Figure index.....	vii
Table index	x
List of abbreviations, symbols and acronyms	xi
1 Introduction	- 1 -
1.1 Chiral Psychoactive drugs as environmental contaminants	- 1 -
1.1.1 Environmental occurrence and ecotoxicity.....	- 3 -
1.2 MDMA.....	- 5 -
1.3 Enantioseparation of chiral drugs	- 7 -
1.4 Ecotoxicity assays.....	- 8 -
1.4.1 Daphnia as an invertebrate model in ecotoxicity	- 9 -
1.4.2 Morphophysiological and reproduction endpoints.....	- 10 -
1.4.3 Behavioural endpoints	- 11 -
1.4.4 Biochemical endpoints	- 11 -
2 Aims.....	- 13 -
3 Materials and methods	- 14 -
3.1 Enantioseparation of MDMA	- 14 -
3.1.1 Chemicals and materials.....	- 14 -
3.1.2 Equipment and chromatographic conditions	- 14 -
3.2 Ecotoxicity assays.....	- 16 -
3.2.1 Equipment and reagents.....	- 16 -
3.2.2 Preparation of culture medium and daphnia maintenance.....	- 16 -
3.2.3. Preparation of <i>Raphidocelis subcapitata</i> microalgae culture medium.....	- 17 -
3.2.4 Experimental design	- 18 -
3.2.5 Morphophysiological parameters.....	- 20 -

3.2.6 Swimming behaviour.....	- 21 -
3.2.7 Reproduction parameters	- 23 -
3.2.8 Biochemical parameters.....	- 23 -
3.3 Statistical Analysis.....	- 25 -
4 Results and Discussion	- 26 -
4.1 Multimilligram enantioresolution of MDMA	- 26 -
4.1.1 Injection volume optimization	- 26 -
4.1.2 Enantioseparation	- 27 -
4.1.3 Enantiomeric purity analysis.....	- 29 -
4.1.4 Quantification/recovery of enantiomers	- 31 -
4.2 Ecotoxicity assays.....	- 33 -
4.2.1 Morphophysiological parameters.....	- 33 -
4.2.2 Swimming behaviour.....	- 36 -
4.2.3 Reproduction parameters	- 38 -
4.2.4 Biochemical parameters.....	- 39 -
5 Conclusions and future perspectives.....	- 42 -
6 Bibliographic references	- 43 -
7 Attachments.....	I
Annex I – Abstract and Poster communication presented in APCF-TOXRUN International Congress 2022.....	I
Annex II – Stock solutions for preparation of <i>R. subcapitata</i> culture medium.....	III
Annex III – Preparation of standards and samples for biochemical assays.....	III

Figure index

Figure 1 Sources of pharmaceuticals and illicit drugs as environmental contaminants.-	3
-	
Figure 2 Chemical structure of MDMA enantiomers. <i>S</i> (+)-MDMA in the left and <i>R</i> (-)-MDMA in the right.	6
Figure 3 Morphology and anatomy of an adult <i>D. magna</i> with eggs. (A) diagram of adult daphnia anatomy (with authors permission, Ondina Ribeiro and João Carrola); (B) photography of adult daphnia (barr=1mm).	9
Figure 4 Illustration of <i>D. magna</i> life cycle. Blue arrows represent sexual reproduction and green arrows represent asexual reproduction (with authors permission, Ondina Ribeiro and João Carrola).....	10
Figure 5 Algae culture medium, in magnetic agitation, with 2 Teflon tubes: 1-tube for airflow out, 2-tube with filtered air supply with a 0.22 µm filter that connects to an air pump system.	18
Figure 6 (A) Schematic representation of the toxicity assay with a control group and three different concentrations of (<i>R,S</i>)-MDMA, 5 replicates of each group. (B) Photo of the toxicity assay with (<i>R,S</i>)-MDMA, showing the arrangement of flasks with 200 mL of MRHW medium each.	19
Figure 7 Schematic representation of the experimental design. Error! Bookmark not defined.	
Figure 8 Optical microscope coupled to the digital camera to video recording to assess morphophysiological parameters using specific software.....	20
Figure 9 Digimizer program layout with body size, heart area and size measurements.-	21
Figure 10 Equipment used for video record of daphnia swimming behaviour.	22
Figure 11 DaVinci Resolve 17 (in the left) and The Real Fish Tracker (0.4.0) (in the right) programs used for swimming behavioural determinations.....	22
Figure 12 Chromatogram showing the separation of (<i>R,S</i>)-MDMA enantiomers [<i>R</i> (-)-MDMA and <i>S</i> (+)-MDMA] in semi-preparative amylose 3,5-dimethylphenylcarbamate column by LC-DAD at normal phase. Mobile phase: <i>n</i> -Hex (0.1% DEA) and EtOH (0.1%DEA), 80:20 v/v; flow-rate: 1.5 mL/min; detector:210 nm; injection volume: 5 µL. Standard solution at 1 mg/mL (EtOH).	26

Figure 13|Chromatogram showing the injection volume optimization for the enantioseparation of (*R,S*)-MDMA in semi-preparative amylose 3,5-dimethylphenylcarbamate column by LC-DAD at normal elution mode. Mobile phase: *n*-Hex (0.1% DEA) and EtOH (0.1% DEA), 80:20 *v/v*; flowrate: 1.5mL/min; detector: 210 nm. Standard solution at 30 mg/mL (EtOH) and injection volume Line a) 5 μ L; line b) 10 μ L; line c) 15 μ L; and line d) 20 μ L.....- 27 -

Figure 14| Chromatogram showing the separation of MDMA enantiomers [*R*(-)-MDMA and *S*(+)-MDMA)] in the semi-preparative amylose 3,5-dimethylphenylcarbamate column by LC-DAD at normal elution mode. Mobile phase: *n*-Hex (0.1% DEA) and EtOH (0.1% DEA), 80:20 *v/v*; flowrate: 1.5 mL/min; detector: 210 nm; injection volume: 20 μ L. Standard solution at 30 mg/mL (EtOH). The red dotted line corresponds to the cut-off time, that is, the time when each enantiomeric fraction was collected in the respective flask. The fraction corresponding to *R*(-)-MDMA was collected from 9 minutes to 11 minutes, the intermediate fraction was collected from 11 minutes to 11.5 minutes and the fraction corresponding to *S*(+)-MDMA was collected from 11.5 to 15 minutes.- 28 -

Figure 15| Chromatogram showing the separation of MDMA enantiomers [*R*(-)-MDMA and *S*(+)-MDMA)] in the semi-preparative amylose 3,5-dimethylphenylcarbamate column by LC-DAD at normal elution mode. Mobile phase: *n*-Hex (0.1% DEA) and EtOH (0.1% DEA), 80:20 *v/v*; flowrate: 1.5mL/min; detector: 210 nm; injection volume: 100 μ L of intermediate fraction. The red dotted line corresponds to the cut-off time, that is, the time when each enantiomeric fraction was collected in the respective flask. The fraction corresponding to *R*(-)-MDMA was collected from 9 minutes to 11.5 minutes and the fraction corresponding to *S*(+)-MDMA was collected from 11.5 minutes to 15 minutes.- 28 -

Figure 16|Chromatogram and absorption spectra (absorbance scale: 0.240) showing *R*(-)-MDMA and *S*(+)-MDMA fraction analysis in the semi-preparative amylose 3,5-dimethylphenylcarbamate column by LC-DAD at normal elution mode. Mobile phase: *n*-Hex (0.1% DEA) and EtOH (0.1% DEA), 80:20 *v/v*; flow-rate: 1.5 mL/min; detector: 210 nm; injection volume: 100 μ L. Legend: Chromatogram representing *R*(-)-MDMA fraction in line a/red (absorption spectra above) and and *S*(+)-MDMA fraction in line b/black (absorption spectra below).- 30 -

Figure 17|Chromatogram showing the separation of MDMA enantiomers in the analytical column (Lux® 3 μ m i-Amylose-3 column) in reversed elution mode. Mobile

phase: EtOH and UPW with 0.1% DEA; flowrate: 0.1mL/min; detector:210 nm; injection volume: 10 µL. Standard solution at 100 µg/mL(EtOH). Legend: Black line - EtOH and UPW with 0.1% DEA (65:35, v/v), and Pink line - EtOH and UPW with 0.1% DEA (70:30, v/v).....- 32 -

Figure 18|Morphophysiological effects of racemic MDMA determined at day 3 (in the left panel) and day 8 (in the right panel). Note: Asterisks (*) represent significant differences relatively to the control.- 34 -

Figure 19|Morphophysiological effects of MDMA enantiomers determined at day 3 (in the left panel) and day 8 (in the right panel). Note: Asterisks (*) represent significant differences relatively to the control.- 35 -

Figure 20|Swimming behaviour effects of MDMA racemate (in the left panel) and enantiomers (in the right panel), determined at day 5. Note: Asterisks (*) represent significant differences relatively to the control.- 37 -

Figure 21|Effects of MDMA racemate (in the left panel) and enantiomers (in the right panel) on *D. magna* reproduction.- 39 -

Figure 22|Effects of MDMA racemate (in the left panel) and enantiomers (in the right panel), on biochemical parameters. Note: Asterisks (*) represent significant differences relatively to the control.- 40 -

Table index

Table 1 Percentage of drug use (DU%) by european adults (15-64 years old) and purity (%) in 2021 (EMCDDA 2022).	- 1 -
Table 2 Environmental occurrence and ecotoxicity of psychoactive substances.	- 4 -
Table 3 Preparation of samples for MDA determination.	- 25 -
Table 4 Chromatographic conditions optimization for the recovery determination of MDMA enantiomers.	- 31 -
Table 5 Results of MDMA enantiomers recovery obtained by semi-preparative chromatography.	- 32 -
Table 6 Statistical analysis of morphophysiological effects of MDMA racemate and enantiomers on <i>D. magna</i> , determined at day 3 and 8. Significant effects ($p < 0.05$) in bold.....	- 36 -
Table 7 Statistical analysis of swimming behaviour effects of MDMA racemate and enantiomers on <i>D. magna</i> , determined at day 5. Significant effects ($p < 0.05$) in bold.-	38 -
Table 8 Statistical analysis of effects of MDMA racemate and enantiomers on <i>D. magna</i> reproduction.....	- 39 -
Table 9 Statistical analysis of biochemical effects of MDMA racemate and enantiomers on <i>D. magna</i> . Significant effects ($p < 0.05$) in bold.	- 41 -
Table 10 Preparation of standards for BSA calibration curve.	III
Table 11 Preparation of standards for DCF calibration curve.	IV
Table 12 Preparation of standards and samples for CAT activity.....	IV
Table 13 Preparation of standards for MDA calibration curve.....	V

List of abbreviations, symbols and acronyms

- AChE** Acetylcholinesterase
- AMP** Amphetamine
- AMT** Ammonium molybdate tetrahydrate
- ATCI** Acetylthiocholine iodide
- BE** Benzoyllecgonine
- BHT** Butylated hydroxytoluene
- B₁** Thiamine
- B12** Cyanocobalamin
- CAT** Catalase
- CE** Capillary electrophoresis
- CNS** Central nervous system
- COC** Cocaine
- CSPs** Chiral stationary phases
- DCF** 2,7-dichlorofluorescein
- DCFH** Dichlorofluorescein
- DEA** Diethylamine
- DMSO** Dimethyl sulfoxide
- DNTB** 5,5'-dithiobis (2-nitrobenzoic acid)
- EF** Enantiomeric Fraction
- EMCDDA** European Monitoring Centre for Drugs Addiction
- EtOH** Ethanol
- EU** European Union
- FDA** Food and Drug Administration
- GC** Gas chromatography
- H** Biotin
- HPLC-DAD** High-performance liquid chromatographic with a diode array detector
- IPA** Isopropanol
- ISO** International Organization for Standardization
- K** Ketamine
- LC** Liquid chromatography
- MAPS** Multidisciplinary Association for Psychedelic Studies
- MDMA** 3,4-methylenedioxymethamphetamine

MDA Malondialdehyde

MDPV Methylenedioxypropylone

MeOH Methanol

MHRW Moderately Hard Reconstituted Water

NK Norketamine

NPS New Psychoactive Substance (uniformizar a escrita)

OECD Organisation for Economic Cooperation and Development

PBS Phosphate Buffer Solution

PTSD Post Traumatic Stress Disorder

ROS Reactive Oxygen Species

SDS Sodium Dodecyl Sulphate

TBA Thiobarbituric acid

TBARS Thiobarbituric Acid Reactive Substances

TCA Trichloroacetic acid

TNB 5-thio-2-nitrobenzoic acid

UPW Ultrapure Water

WWTP Wastewater Treatment Plants

1| Introduction

1.1| Chiral Psychoactive drugs as environmental contaminants

The high and growing consumption of drugs, in particular psychoactive substances (PAS), continues to be a problem with great impact on public health (EMCDDA 2022). Drugs have the potential to develop addiction and, consequently, trigger illicit uses, since they act on the central nervous system (CNS) temporarily altering consciousness, perception and mood (Dinis-Oliveira 2014). The way they interact with the CNS allows them to be divided into several classes of drugs: stimulants, hallucinogens and depressants (Dinis-Oliveira 2014; Jin et al. 2022). Still, the continuous emergence of New Psychoactive Substances (NPS) is a matter of great concern. NPS appeared on the market in 2005, peaked in 2014 and, since 2015, about 400 NPS are reported every year in Europe (EMCDDA 2022; OEDT 2021). According to the European Monitoring Centre for Drugs and Drug Addiction (EMCDDA), in recent years, the volumes of cocaine and heroin entering the European Union (EU) and the production of drugs, in particular synthetic drugs (amphetamines and ecstasy), have reached an all-time high. In addition, the European drug market has provided a diverse range of drugs of increasingly higher purity. Cannabis (CNN), cocaine (COC), 3,4-methylenedioxymethamphetamine (MDMA) and amphetamines (AMPs) seem to be the most used drugs by adults. **Table 1** shows the most recent data on the consumption and purity of the most common drugs used by european population aged 15 to 64 years (EMCDDA 2022).

Table 1| Percentage of drug use (DU%) by european adults (15-64 years old) and purity (%) in 2021 (EMCDDA 2022).

Drug	DU (%)	Purity (%)
CNN	7.7	-
COC	1.2	54-68
MDMA	0.9	62-83
AMPs	0.7	20-37
NPS	0.6	-

AMPs - amphetamines; CNN – cannabis; COC – cocaine; MDMA – 3,4-methylenedioxymethamphetamine; NPS – new psychoactive substances.

Many illicit drugs are chiral, a three-dimensional molecule with asymmetry in their structures that cannot be superimposed on their mirror image. The asymmetry may be

due the presence of stereogenic centers, most often a carbon bonded to four different groups (Tiritan et al. 2016). Those structures that cannot be superimposed on their mirror image are called enantiomers. These molecules exhibit similar thermodynamic and spectrometric properties; however, they can be distinguished by the conventional method of rotating plane polarized light: rotation to the right (clockwise) is called dextrorotatory (+), and rotation to the left (counterclockwise) is called levorotatory (-). The spatial orientation of the substituents of the stereogenic center (configuration), are designated as *R* (from Latin *rectus*, in English right) or *S* (from Latin *sinister*, in English left). Further, racemate is the name given to the equimolar mixture of both enantiomers (Ribeiro et al. 2018; Tiritan et al. 2016).

Biological systems, like living organisms, are intrinsically chiral. Despite the similarity that enantiomeric structures can reveal in terms of thermodynamic properties in an achiral environment, enantiomers can exhibit different pharmacokinetic and pharmacodynamic properties in a chiral environment, including toxicity. This is due to the enantioselective interaction with macromolecules present in living organisms (Fontes, Maranhão, and Pereira 2020; Pérez-Pereira et al. 2022; Tiritan et al. 2016).

Illicit drugs can be available either as racemates or as a single enantiomer. However, after consumption, the drug may undergo enantioselective metabolism and both parent and metabolites can be excreted in different enantiomeric proportions (Jin et al. 2022; Kaushik and Thomas 2019). Regarding the life cycle of drugs, whether pharmaceutical or illicit, their final destination is the aquatic environment as a result of direct discharges of sewage after consumption, clandestine laboratories or from Wastewater Treatment Plants (WWTPs), which biodegradation by microbiological processes do not have the capacity to completely eliminate these substances. The consequent increase in their release into the environment makes these substances a group of environmental contaminants of growing concern (**Figure 1**) (Barreiro, Tiritan, and Cass 2021; Emke et al. 2014; Evans, Bagnall, and Kasprzyk-Hordern 2016, 2017; Hernández et al. 2014; Jin et al. 2022; Mackul'ak et al. 2016; Nilsen et al. 2019; Pérez et al. 2005; Ribeiro et al. 2020).

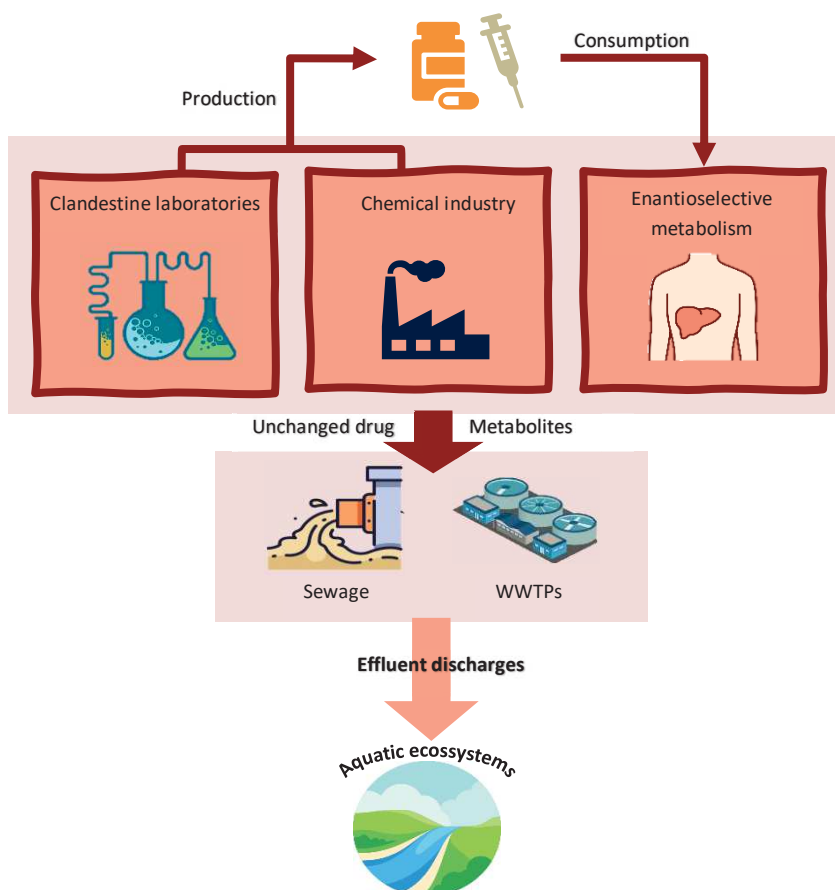


Figure 1| Sources of pharmaceuticals and illicit drugs as environmental contaminants.

1.1.1| Environmental occurrence and ecotoxicity

PAS have been widely detected in wastewater and surface waters. Monitoring studies have been carried out all over the world (De Felice et al. 2019; Fraz et al. 2019; Nilsen et al. 2019; Ribeiro et al. 2017; Ribeiro, Ribeiro, and Tiritan 2016), mostly to estimate their consumption and few studies estimate the ecotoxicity. However, the impacts of single enantiomers on non-target organisms are often neglected.

Even at low concentrations (ng L^{-1} to $\mu\text{g L}^{-1}$), PAS have the potential to accumulate in aquatic food webs and/or interfere with physiological, reproductive, biochemical and behavioural processes of aquatic organisms causing adverse effects on non-target organisms (De Felice et al. 2019; Fraz et al. 2019; Nilsen et al. 2019; Ribeiro et al. 2017, 2016). Table 2 presents the occurrence of some PAS in surface waters and wastewaters around the world. The enantiomeric fractions (EF) reported, and the effects of the drugs are also described.

Table 2 | Environmental occurrence and ecotoxicity of psychoactive substances.

Drug	Surface water (ng L ⁻¹)	Wastewater (ng L ⁻¹)	EF	Toxicity effects
COC	6.0 (Baker and Kasprzyk-Hordern 2011); 3.4±0.8 (Skees et al. 2018)	29.2 (Baker and Kasprzyk-Hordern 2011); 19.4±12.6 (Skees et al. 2018); 14.8 (Baker and Kasprzyk-Hordern 2013); 8 (Hubert et al. 2017)	-	COC induces overproduction of reactive oxygen species and affects swimming behaviour and causes changes in the development of <i>Daphnia magna</i> (De Felice et al. 2019).
BE	26.8 (Baker and Kasprzyk-Hordern 2011); 14.2±10.0 (Skees et al. 2018)	115.9 (Baker and Kasprzyk-Hordern 2011); 31.5±14.5 (Skees et al. 2018); 61.8 (Baker and Kasprzyk-Hordern 2013); 44 (Hubert et al. 2017)	-	BE concentrations similar to those found in the aquatic ecosystems (50 and 500 ng L ⁻¹) are capable of inducing oxidative stress, inhibiting AChE activity, and affecting swimming behaviour and the development of <i>D. magna</i> (Parolini et al. 2018).
AMPH	0.5-1.4 (Li et al. 2016)	21.8±18.1 (Skees et al. 2018); 1.5-3.8 (Baker and Kasprzyk-Hordern 2013)	-	Exposure to AMPHs at a concentration of 5000 ng L ⁻¹ triggered an overproduction of reactive oxygen species that led to oxidative and genetic damage in the bivalve <i>Dreissena polymorpha</i> (Parolini et al. 2016).
METH	86.4±64.3 (Skees et al. 2018); 350.1±78.3 (Bartelt-Hunt et al. 2009)	125±32.8 (Skees et al. 2018); 0.8 (Baker and Kasprzyk-Hordern 2013); 28.0 (Evans et al. 2015); 22 (Hubert et al. 2017)	0.5 (Evans et al. 2015)	Low concentrations of METH (50 and 500 ng L ⁻¹) affected the oxidative status and the development of <i>D. magna</i> (De Felice et al. 2020).
MDMA A	8.7 (Baker and Kasprzyk-Hordern 2011); 6.1±0.3 (Skees et al. 2018); 60 (Evans et al. 2017)	37.5 (Baker and Kasprzyk-Hordern 2011); 13.4 (Baker and Kasprzyk-Hordern 2013); 45.3±0.5 (Evans et al. 2015); 45.3 (Evans et al. 2015)	0.9 (Evans et al. 2015) 0.71 (Kasprzyk-Hordern, Kondakal, and Baker 2010) <0.3 (Evans et al. 2017) ~1 (Gonçalves et al. 2019)	High doses of MDMA (40-120 mg L ⁻¹) reduced bottom swimming and immobility and conferred habituation in <i>D. rerio</i> (Stewart et al. 2012).
K	-	75±1.9 (Lin, Lee, and Wang 2014); 82±11-166±12 (Adhikari et al. 2022)	-	High concentrations of KET (>100 µg L ⁻¹) increase mortality and caused enantioselective toxicity effects in <i>D. magna</i> (Li, Wang, and Lin 2017; Pérez-Pereira et al. 2022).
NK	0.4-6.5 (Li et al. 2016)	0.6-12.0 (Baker and Kasprzyk-Hordern 2013); 110±3.0 (Lin et al. 2014)	-	NK caused toxicity effects in <i>D. magna</i> (Pérez-Pereira et al. 2022).
MDPV	1.4-1.6 (Fontanals, Marcé, and Borrull 2017)	2.8-25.0 (Fontanals et al. 2017)	-	-

BE – benzoylecgonine; COC – cocaine; MDMA - 3,4-methylenedioxymethamphetamine; METH –methamphetamine; K – Ketamine; AMPH – amphetamine; NK – norketamine; MDPV - methylenedioxypyrovalerone

1.2| MDMA

The 3,4-methylenedioxyamphetamine (MDMA), a synthetic derivative of amphetamine, is a PAS that ranks in the third place among recreational drugs in Europe. The availability of MDMA ecstasy pills has been a constant concern of the competent authorities (Anon 2014; EMCDDA 2020). This substance has a stimulating action on the CNS and can induce unique psychopharmacological effects, such as a decrease in fear and an increase in well-being, sociability, interpersonal trust, acceptance of oneself and others, and ability to approach these problems without extreme disorientation or loss of ego due to the alert state of consciousness (Feduccia and Mithoefer 2018). These factors might provide the opportunity for a corrective emotional experience (Cruz et al. 2020; Feduccia and Mithoefer 2018).

In 2017, the Multidisciplinary Association for Psychedelic Studies (MAPS) supported a clinical trial for possible Food and Drug Administration (FDA) approval of the use of MDMA in the treatment of Post-Traumatic Stress Disorder (PTSD). PTSD affects more than 350 million of people worldwide. This increasingly common disease is triggered by a traumatic event experienced or witnessed, and negatively affects daily life regarding cognitive and psychosocial functioning, relationships, increased depression, among others, and may increase suicidal tendencies. The trial has recently progressed to the second of two Phase 3, after Phase 1, Phase 2 and first Phase 3 trials showed promising results in mitigating PTSD (Cruz et al. 2020; Feduccia, Holland, and Mithoefer 2018; Feduccia and Mithoefer 2018; Mitchell et al. 2021; Mithoefer 2017; Sessa 2017). MDMA, when taken in moderate doses for a limited time (2 or 3 administrations) can be safe and useful in the treatment of PTSD since its capable of inducing unique psychopharmacological effects (Feduccia and Mithoefer 2018; Mithoefer et al. 2013, 2018; Sessa 2017). Furthermore, the study carried out by Mithoefer et al. (2013) demonstrated a long-term durability of PTSD symptom reduction, averaging 3.5 years after ending MDMA-assisted psychotherapy. As this drug is known to increase feelings of confidence and for the fact that it confers fast-acting therapeutic effects without the need for daily dosing or a steady state to maintain its effectiveness, it is believed to be an ideal adjunct to psychotherapy. It is estimated that the study will end this year and the therapy could be implemented in 2023 or 2024 (Cruz et al. 2020; MAPS n.d.; Mithoefer et al. 2013; Sessa 2017).

Although this substance is sold in illicit markets in the form of a racemate, a mixture of 50% of each enantiomer (*S*(+)-MDMA and *R*(-)-MDMA) (**Figure 2**), it should be considered that its metabolization is enantioselective (Pizarro et al. 2003, 2004). Thus, MDMA and its metabolites are excreted in different enantiomeric proportions. In fact, after consumption, the *S*(+)-MDMA enantiomer is more rapidly metabolized leading to an enrichment of the *R*(-)-enantiomer in the urine and later in the environment (Cruz et al. 2020; Emke et al. 2014; Evans et al. 2016; Ribeiro et al. 2018). Enantioselective metabolism has been used in the context of wastewater based epidemiology to distinguish between consumption and direct disposal with forensic implications (Emke et al. 2014; Evans et al. 2015; Ribeiro et al. 2018; Vazquez-Roig et al. 2014). Additionally, the biological degradation processes in WWTP are also enantioselective with consequent discharge to the effluent receiving systems in different enantiomeric fractions (Cruz et al. 2020; EMCDDA 2020). MDMA enantiomers may have different biological activities (toxicity and potency). Therefore, it is highly relevant its enantioselectivity in ecotoxicity, for a correct assessment of environmental and public health risks (Cruz et al. 2020).

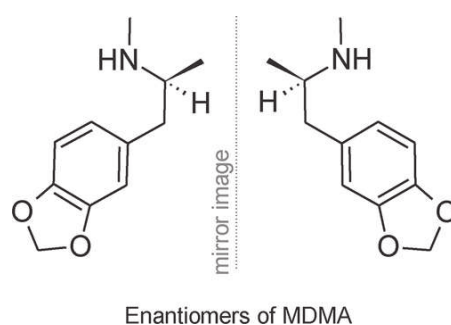


Figure 2 | Chemical structure of MDMA enantiomers. *S*(+)-MDMA in the left and *R*(-)-MDMA in the right.

Several studies have reported the presence of this biologically active substance in surface waters, wastewater (Chen et al. 2021; Emke et al. 2014; Evans et al. 2016; Hernández et al. 2014; Huerta-Fontela, Galceran, Martin-Alonso, et al. 2008; Karolak et al. 2010; Mackuľak et al. 2016) and drinking water (Chen et al. 2021; Evans et al. 2016; Kaushik and Thomas 2019). Chemical analysis of wastewater from 42 European cities in 2017 and 2018 revealed an increase in the prevalence of MDMA detection, which points to an increase in the consumption of this substance and/or its purity (EMCDDA 2020). MDMA and its metabolites have been found at concentrations levels that may negatively interfere with ecosystems (EMCDDA 2020; Mackuľak et al. 2016; OEDT 2021). Additionally, MDMA removal rates are generally poor and can range from 12% to 88% considering

the studies of Huerta-Fontela et al. (2008), Bijlsma et al.(2012), Baker and Kasprzyk-Hordern (2013) and Evans et al. (2016). Some studies reported the occurrence of MDMA enantiomers in aquatic environments and WWTP effluents, with a predominance of the *R*(-)-enantiomer, due to its lower metabolization compared to *S*(+)-MDMA (Baker and Kasprzyk-Hordern 2011; Evans et al. 2016; Vazquez-Roig et al. 2014).

1.3| Enantioseparation of chiral drugs

Environmental studies on chiral PAS have proved to be an important tool for estimating environmental risk and promoting environmental protection measures. However, there are only a few studies regarding the enantioselective environmental occurrence and its ecotoxicological effects. In fact, the methodology to quantify and identify enantiomers is challenging due to the identical thermodynamic and spectrometric properties of these structures (Barreiro et al. 2021; Ribeiro et al. 2020; Tiritan et al. 2016). However, great advances have been made in the field of analytical chromatographic enantioseparation methodologies, such as liquid chromatography (LC), gas chromatography (GC), capillary electrophoresis (CE), among others. LC is the method of choice due to its advantages such as speed, high sensitivity, and reproducibility (Bade et al. 2019; Jin et al. 2022; Ribeiro et al. 2018, 2020; Salgueiro-González et al. 2019; Tiritan et al. 2016).

Pure enantiomers can be obtained in two ways: from the preparative resolution of the racemate, or by enantioselective synthesis of the enantiomer of interest. However, the racemic approach is the preferential technique since it provides both enantiomers with high enantiomeric purity for further studies (Ribeiro et al. 2020; Tiritan et al. 2016).

The racemate resolution can be achieved by LC which can be acquired by the indirect method or by the direct method. The indirect method is more demanding because the compound in the racemate form reacts with an enantiomerically pure reagent to form a pair of diastereoisomers, which can be separated by conventional purification methods, and the enantiomers can be recovered by overturning the derivatization procedure. Preparative chromatography using chiral stationary phases (CSPs) has been the most efficient tool in enantiomeric separation, allowing a range of alternatives to the indirect method. Enantioresolution by direct method offers several advantages in both preparative and analytical chromatography, as it does not require derivatization, requires less sample handling, and allows faster results. CSPs consist of a chiral selector adsorbed or chemically linked to a solid support that will preferentially interact with one of the

enantiomers of the mixture and lead to the formation of transitory diastereoisomeric complexes with different stability. This difference in stability is reflected in different retention times, in which the enantiomer that forms the least stable complex is the first to elute. LC with CSPs has been useful in determining the enantiomeric fractions of various drugs in various types of matrices, and the choice of stationary phase is based on experience, literature knowledge, analyte, selector characteristics and trial-error (Ribeiro et al. 2018, 2020; Teixeira et al. 2019; Tiritan et al. 2016).

There are different elution modes of chiral chromatography. Reversed elution mode consists in using a mobile phase with polar characteristics, mainly water and polar organic solvent. The normal elution mode uses nonpolar solvents such as hexane with polar organic solvents (e.g., isopropanol or ethanol). Polar organic elution mode uses only polar organic solvents (acetonitrile, methanol, ethanol, propanol, and their mixtures). Finally, the polar ionic mode consists in the mixture of polar organic solvents with acid or base or soluble volatile salts (e.g., ammonium acetate). The polar ionic elution mode is required when the target analyte has ionizable groups (Nehate et al. 2018; Petrie et al. 2018; Zhao et al. 2018). The normal and polar elution modes are useful for preparative separation because of easier solvent evaporation and the high solubility of polar analyte in these eluents (Cass and Batigaglia 2003; Tachibana and Ohnishi 2001).

1.4| Ecotoxicity assays

Chronic exposure to low concentrations of environmental contaminants may not cause obvious toxicity (e.g., mortality), but interfere with other key endpoints such as the cellular, biochemical, physiological and behavioural processes of non-target organisms (Kaushik and Thomas 2019; Nilsen et al. 2019; Tkaczyk et al. 2021). In addition, environmental pollutants exist as mixtures and thus, interfere with or potentiate harmful effects. Some standardized protocols have been developed by international organizations - such as Organisation for Economic Cooperation and Development (OECD) and International Organization for Standardization (ISO) – for the assessment of acute or chronic toxicity effects of contaminants and to adapt them to include other biomarkers of toxicity.

1.4.1| *Daphnia* as an invertebrate model in ecotoxicity

The freshwater microcrustacean, *D. magna*, is an ecologically relevant organism as is a basic element of food webs, and its presence/absence can provide valuable information about the disturbance of aquatic ecosystems. Therefore, this sensitive organism has been used by the regulatory authorities for ecotoxicity studies (OECD 2004; Ribeiro et al. 2021; Tkaczyk et al. 2021).

Daphnia is a planktonic microcrustacean found in freshwater lentic aquatic ecosystems, with temperatures between 18-22°C. It has a transparent exoskeleton composed of chitin and is approximately 5 millimetres long. It has two compound eyes with ommatidia for light detection, a small simple eye (ocellus), two pairs of antennae – the first with a sensory function and the second with a swimming function - and 4-6 pairs of thoracic limbs. Males are smaller than females and have larger first antennae. Morphological and anatomical characteristics of *D. magna* are represented in **Figure 3**. They feed essentially on fine particles of suspended organic matter, including yeasts and microalgae. In addition to being an ecologically relevant organism, *daphnia* has several advantages such as: it is relatively easy to maintain and handle and have a short life cycle producing a high number of descendants. Furthermore, the transparent exoskeleton allows the evaluation of several morphophysiological parameters with non-invasive methods, like a loupe or microscope (Antunes and Castro 2017; Ribeiro et al. 2021; Tkaczyk et al. 2021).

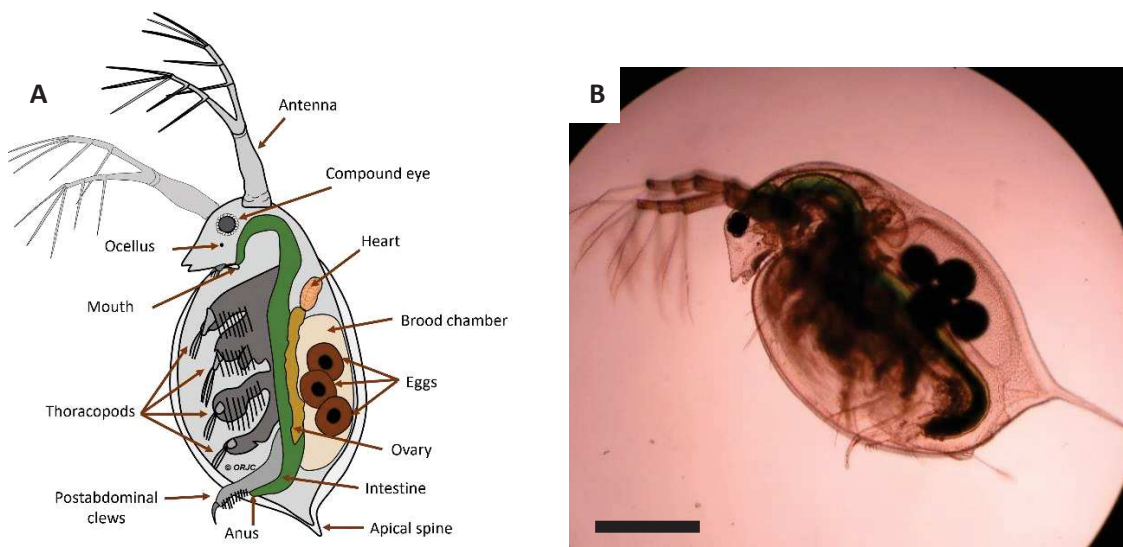


Figure 3|Morphology and anatomy of an adult *D. magna* with eggs. **(A)** diagram of adult daphnia anatomy (with authors permission, Ondina Ribeiro and João Carrola); **(B)** photography of adult daphnia (barr=1mm).

These organisms can reproduce either sexually or asexually (apomixis). Under favourable environmental conditions, daphnia reproduces asexually, leading to the production of diploid eggs that produce juvenile females genetically identical to the parent (reproduction by parthenogenesis). This type of reproduction is important in ecotoxicological studies as it guarantees the homogeneity of organisms, reducing the variability of results. Under adverse conditions and in the presence of males, they fertilize sexual eggs, giving rise to haploid eggs that have a resistant protective membrane - ephippia/resistance eggs - and do not develop until environmental conditions are favourable. Only at this point, resistance eggs can hatch to give rise to neonates. Sexual reproduction results in the production of males and females with increased genetic variability (Antunes and Castro 2017; Campos et al. 2018; Ribeiro et al. 2021; Tkaczyk et al. 2021). Neonates from the first two broods are less resistant. The 3rd-4th generation daphnia neonates are more resistant and ideally used in ecotoxicity assays. **Figure 4** shows the sexual and asexual life cycle of *D. magna*.

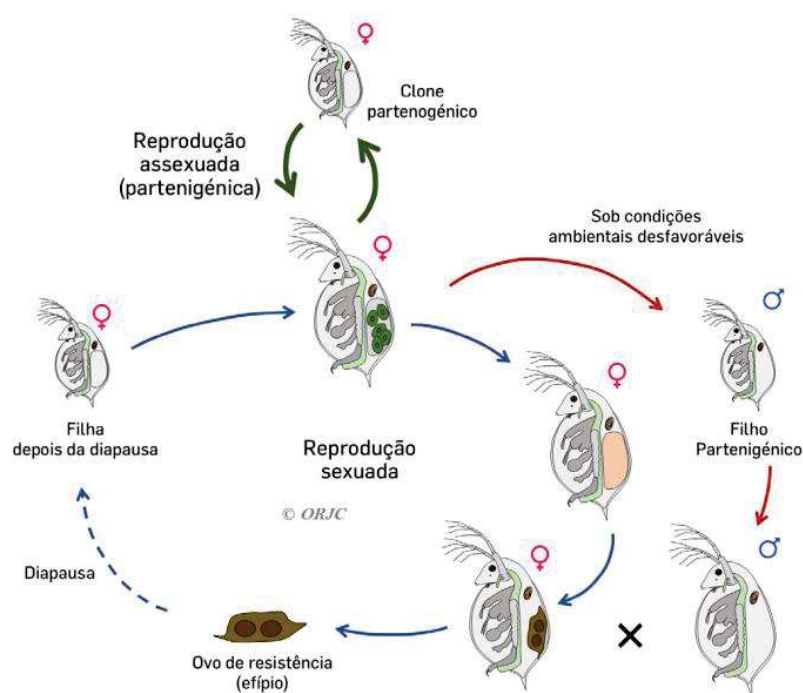


Figure 4 Illustration of *D. magna* life cycle. Blue arrows represent sexual reproduction and green arrows represent asexual reproduction (with authors permission, Ondina Ribeiro and João Carrola).

1.4.2| Morphophysiological and reproduction endpoints

Morphophysiological parameters (e.g., body size, feeding rate, heart activity, etc.) and reproduction parameters (e.g., offspring), are indicators of toxicity since they may

manifest earlier than mortality and are sensitive to sublethal concentrations of toxics (Nilsen et al. 2019; Szabelak and Bownik 2021). Microscopic observation is an easy and non-invasive methodology that can be used for the determination of these parameters due to daphnia transparent exoskeleton (Bownik 2020; Szabelak and Bownik 2021).

1.4.3| Behavioural endpoints

Some studies have been showing that swimming behaviour also can be a sensitive biomarker of toxicity. Parameters such as swimming speed, distance travel and active time may be altered due to exposure to contaminants such as PAS (Bownik 2017; Parolini et al. 2018; Stewart et al. 2012; Szabelak and Bownik 2021). Improvement and optimization of visual tools for image and video acquisition, new techniques and the development of software able to process data have been facilitating the complex analysis and understanding the swimming behaviour.

1.4.4| Biochemical endpoints

1.4.4.1| Acetylcholinesterase activity

Acetylcholinesterase (AChE) is a crucial enzyme associated with nerve response and function. This enzyme has been used as a crucial biomarker of contaminants in the nervous system, since its inhibition may lead to muscular paralysis, convulsions, and asphyxia (Lionetto et al. 2013; Rodríguez-Fuentes et al. 2015; Silman and Sussman 2008). Some studies reported that some pharmaceuticals such as diazepam and fluoxetine can inhibit AChE activity in diverse aquatic organisms, including daphnia, leading to neurotransmission impairment (Ding et al. 2017).

1.4.4.2| Reactive oxygen species (ROS)

ROS are unstable molecules (including peroxide – H_2O_2 , superoxide – O_2^- and hydroxyl radical – OH^\cdot) induced by exogenous sources but also produced in the metabolic process of the body and are necessary to organisms, since they are involved in cell growth, proliferation, development, apoptosis and other (Li and Trush 2016; Yang, Chen, and Shi 2019; Yang and Lian 2020). However, excessive ROS occurs when the reduction of oxygen is incomplete and imposes oxidative stress on cells because of a decrease in antioxidant protection, failure to repair oxidative damage, or increase in oxidant generation. The balance between ROS generation and elimination is fundamental to guarantee cell integrity (Li and Trush 2016; Valko et al. 2016; Yang and Lian 2020).

1.4.4.3| Catalase (CAT)

CAT is a cellular antioxidant enzyme that protects against oxidative damage by degrading hydrogen peroxide to water and oxygen (Alfonso-Prieto et al. 2009; Hadwan 2018).

1.4.4.4| Thiobarbituric Acid Reactive Substances (TBARS)

Oxygen free radicals produced by organisms induce lipid peroxidation and the formation of malondialdehyde (MDA, a reactive carbonyl compound). MDA is an indicator of oxidative stress since it can reflect the degree of lipid peroxidation and cell injury (Tsikas 2017).

2| Aims

Studies on the impact of MDMA on aquatic organisms are scarce and there are no studies regarding its enantioselectivity in toxicity on non-target organisms. Considering the possible approval of MDMA-assisted therapy and the low degradation rates of the substance in the form of racemate and enantiomers, it may result in the widespread occurrence of MDMA in the environment, alerting to its possible ecotoxicity. It is essential to investigate its ecotoxicological effects to complement the ecopharmacovigilance data in order to include the entire life cycle of the drug.

The main objectives of this work were to:

- obtain the pure enantiomers of MDMA by semipreparative chromatography, using a previously developed enantioselective method (Gonçalves et al. 2019);
- Investigate the enantioselectivity in the ecotoxicity effects of MDMA using an ecologically relevant aquatic organism, *D. magna*, at different concentrations of MDMA racemate (0.1, 1 and 10 $\mu\text{g L}^{-1}$) and its isolated enantiomers (0.1 and 1 $\mu\text{g L}^{-1}$).

Thus, it was intended to estimate the safety limits of these substances in an environmental context, to support the water quality and environment directive to establish priorities and adopt measures to mitigate the impact of these substances on the environment and, consequently, reduce impacts on food webs and lately for humans.

3| Materials and methods

3.1| Enantioseparation of MDMA

3.1.1| Chemicals and materials

All solvents were of chromatographic grade. Ethanol (EtOH, $\geq 99.8\%$), methanol (MeOH) and isopropanol (IPA) were acquired from Fisher Scientific UK (Leicestershire, United Kingdom); *n*-hexane (*n*-Hex, $\geq 97.0\%$) was acquired from VWR BDH Chemicals (Gliwice, Poland); diethylamine (DEA, 99.5%) was acquired from Sigma-Aldrich (Co, Belgium); Diethyl ether ($\geq 99.7\%$, Sigma-Aldrich); and Hydrogen chloride solution in diethyl ether was acquired from Alfa Aesar (ThermoFisher, Kandel, Germany). Ammonium acetate was purchased from Sigma-Aldrich (Zwijndrecht, Netherlands); ammonium bicarbonate was acquired from Sigma-Aldrich (Darmstadt, Germany); pure anhydrous sodium sulphate 99.7% was acquired from José Manuel Gomes dos Santos, LDA (Odivelas, Portugal). MDMA [(*R,S*)-MDMA, HCl; Ref: MDM-94-HC-50] was acquired from Lipomed (Arlesheim, Switzerland). For semi-preparative chromatography, a MDMA stock solution was prepared in EtOH at a concentration of 30 mg/mL and stored in an amber vial at -20°C .

Ultrapure water (UPW) was obtained from an Ultrapure Water System (SG Ultra Clear UV plus). Microfiber filters with 47 mm and particle retention of 0.7 μm were purchased from VWR®. A Büchi® Rotavapor® R-210 evaporator with vacuum controller (V-850) and water bath (B-491) from BÜCHI SWITZERLAND was used in the evaporation processes.

3.1.2| Equipment and chromatographic conditions

A high-performance liquid chromatographic with a diode array detector equipment (HPLC-DAD) from LaChrom Merck Hitachi®, equipped with an interface system (D-7000), a DAD (L-7455), a pump (L-7100), an autosampler (L-7200) and a data acquisition software (System Manager HSMP-7000, Version 3.0) was used for semipreparative enantioresolution of (*R,S*)-MDMA and enantiomeric purity evaluation. Chromatographic separation was performed according to the method previously developed by Gonçalves et al. (2019). The CSP used was a *tris*-3,5-dimethylphenylcarbamate amylose coated with APS-Nucleosil (500 A, 7 μm , 20%, w/w;

20 x 0.7 cm internal diameter). The analysis was performed under normal elution mode, at room temperature and under isocratic conditions with a flow rate of 1.5 mL/min and the DAD detector adjusted to a wavelength of 210 nm. The mobile phase for the separation of the enantiomers was prepared by mixing *n*-Hex with 0.1% DEA and EtOH with 0.1% DEA (80:20, v/v). Enantiomeric fractions were collected into round-bottomed flasks corresponding to the first enantiomer eluted, an intermediate fraction, and the second enantiomer eluted. The intermediate fraction containing the mixture of both enantiomers was reinjected to allow obtaining a better yield and purity of each enantiomer. Fractions were evaporated using a Büchi® Rotavapor® R-210 and then, reconstituted in 1 mL of EtOH and stored in 2 mL amber vials. The solution was evaporated to dryness in a water bath at ~35-37°C, solubilized in IPA followed by precipitation with HCl in ether dropwise and diethyl ether (enantiomers that were in the free base form were converted into the respective hydrochlorides). The procedure was repeated several times to achieve the maximum recovery of the enantiomers. The precipitate was collected and reconstituted in EtOH.

The enantiomeric purity of the fractions was evaluated using the same equipment and chromatographic conditions. Enantiomeric ratio (e.r) was calculated according to our previous works (Pérez-Pereira et al. 2022; Tiritan et al. 2018) and the following formula:

$$\% e. r. = \frac{Ex \text{ (or } Ey)}{(Ex+Ey)} \times 100, Ex \text{ corresponds to the concentration of the } S(+)\text{-enantiomer}$$

and *Ey* to the concentration of *R*(-)-enantiomer.

Various mobile phases and chromatographic conditions were tested to determine the yield of the collected enantiomeric fractions. The optimized analytical chromatography conditions were achieved using a Shimadzu UFLC Prominence system equipped with a column oven (CTO-20AC), a system controller (CBM-20A), 2 pumps (LC-20AD), an autosampler (SIL-20AC), a FD (RF-10AXL), a data acquisition software LC Solution, version 1.24 SP1 (Shimadzu Corporation, Tokyo, Japan) and a Shimadzu SPD-20A UV/Vis detector coupled to the LC system; Lux® 3µm i-Amylose-3 column (LC Column 150 x 2.0 mm) as CSP; a mixture of EtOH and UPW with 0.1% DEA ,70:30, v/v as the mobile phase (reversed elution mode); a UV detector at 210 nm; flow-rate of 0.1 mL/min; and sample injection volume of 10 µL. All mobile phases were previously filtered using a glass microfibers filter with 0.7 µm porous size.

3.2| Ecotoxicity assays

3.2.1| Equipment and reagents

An autoclave from PBI (South Carolina, USA) and a laminar flow chamber SC4 from Allentown (New Jersey, USA) were used for the preparation and manipulation of solutions and media. The Multiparameter HI98194 and the multiparameter analyser HANNA Consort C863 (Turnhout, Belgium) instruments were used to measure the physical-chemical parameters (pH, conductivity, temperature and percentage of dissolved oxygen (%DO)) of daphnia and microalgae media. Absorbance was measured using an UV/Vis spectrometer (ATI Unicam, Leeds, England). An Inverse Microscope from ZEISS (Jena, Germany) and a Neubauer chamber for microalgae cell counting. A microplate reader, BioTek Synergy 2 (Vermont, USA) was used for biochemical analysis and an ultrasonic of VWR USC-TH (Pennsylvania, USA) for preparation of the daphnia homogenates. A microscope Axiostar plus ZEISS (Jena, Germany) coupled to a digital camera (Canon PowerShot G9) was used for image and videorecording for the morphophysiological and reproductive parameters and a Canon Legria HF R506 was used for swimming video recording for the behaviour assessment.

For biochemical determinations the following reagents were acquired from Sigma-Aldrich (Missouri, USA): Sodium chloride (NaCl); potassium chloride (KCl); disodium phosphate (Na_2HPO_4); potassium dihydrogen phosphate (KH_2PO_4); Coomassie Plus (The Better Bradford Assay™ Reagent); bovine serum albumin (BSA, $\geq 96\%$); UPW; tris base; hydrochloric acid 37%; 5,5'-dithiobis-2-nitrobenzoic acid (DTNB, $\geq 98\%$); acetylthiocholine iodide (ATCI, $\geq 99\%$); 2,7-dichlorofluorescein (DCF, 90%); 2,7-dichlorofluorescein diacetate (H_2DCFDA , $\geq 97\%$); dimethyl sulfoxide (DMSO, $\geq 99.9\%$); monosodium phosphate (NaH_2PO_4 , $\geq 99\%$); ammonium molybdate tetrahydrate (AMT); CAT from *Aspergillus niger* (CAT; ≥ 4.0 units/mg protein; ref. C3515-10MG) at 69629 U/mL ; butylated hydroxytoluene (BHT, $\geq 99\%$); thiobarbituric acid (TBA, $\geq 98\%$); sodium dodecyl sulphate (SDS, $\geq 98.5\%$); trichloroacetic acid (TCA); malondialdehyde (MDA, $\geq 96\%$) from Sigma-Aldrich (St. Louis, EUA or Steinheim, Germany) .

For adjustment of pH, the solutions 6 M of sodium hydroxide (NaOH) and 0.5 M chloridric acid (HCl) were used.

3.2.2| Preparation of culture medium and daphnia maintenance

Organisms were maintained in moderately hard reconstituted water (MHRW) prepared using the following chemicals per liter: 123 mg magnesium sulphate heptahydrate ($\text{MgSO}_4 \cdot 7\text{H}_2\text{O}$, >99%) and 60 mg calcium sulphate dihydrate ($\text{CaSO}_4 \cdot 2\text{H}_2\text{O}$, >99%) obtained from Merck (Darmstadt, Germany); 96 mg sodium bicarbonate (NaHCO_3 , $\geq 99,7\%$) purchased from Sigma-Aldrich (Missouri, USA); 4 mg potassium chloride (KCl , >99%) obtained from Panreac (Barcelona, Spain); The medium was supplemented with: *Ascophyllum nodosum* extract from SOL-PLEX® SIERRA|Alltech (Kentucky, USA); Dried Baker's Yeast from Pura Vida, (Lisbon, Portugal); cyanocobalamin (B12, >98,9%) purchased from Fragon Iberian Laboratory (Oporto, Portugal); biotin (H, $\geq 99\%$) purchased from Panreac AppliChem ITW Reagents (Darmstadt, Germany); and thiamine HCl (B1) purchased from Couto pharmacy manipulation laboratory (Oporto, Portugal). Before being used, the MHRW was aerated for about 30 minutes with an air pump and continuous magnetic agitation. After this time, the physical-chemical parameters were measured: temperature, pH, conductivity and %OD. The medium was then supplemented with 50 μL of stock vitamin mix solution, 9 mL of the *A. nodosum* algae extract stock solution and 500 μL yeast extract per L. Organisms were fed every culture medium change with the microalgae *Raphidocelis subcapitata* at 3.0×10^5 cells/mL for the neonates/juveniles and 6.0×10^5 cells/mL for adults. Groups of 25 daphnids were isolated in 800 mL of medium and maintained as previously referred. Daphnids, less than 24 h old originated from 3rd – 5th brood females from stock cultures were used for new cultures or for the experiments.

3.2.3. Preparation of *Raphidocelis subcapitata* microalgae culture medium

A culture medium composed of macronutrients and micronutrients was prepared according to Annex II with the following chemicals: $\text{MgSO}_4 \cdot 7\text{H}_2\text{O}$, and boric acid (H_3BO_3 , $\geq 99,8\%$) both obtained from Merck (Darmstadt, Germany); manganese(II) chloride hexahydrate ($\text{MnCl}_2 \cdot 4\text{H}_2\text{O}$, $\geq 98\%$) and cobalt(II) chloride hexahydrate ($\text{CoCl}_2 \cdot 6\text{H}_2\text{O}$, >99%) purchased from PA Panreac (Barcelona, Spain); zinc chloride (ZnCl_2 , >97%) and potassium hydrogen phosphate (K_2HPO_4 , >99%) acquired from Panreac AppliChem ITW Reagents (Darmstadt, Germany); sodium nitrate (NaNO_3 , >99%), sodium bicarbonate (NaHCO_3 , $\geq 99,7\%$), sodium molybdate dihydrate ($\text{Na}_2\text{MoO}_4 \cdot 2\text{H}_2\text{O}$, $\geq 98\%$) and disodium EDTA dihydrate ($\text{Na}_2\text{EDTA} \cdot 2\text{H}_2\text{O}$, $\geq 98,5\%$) acquired from Sigma-Aldrich (Missouri, USA); magnesium chloride hexahydrate ($\text{MgCl}_2 \cdot 6\text{H}_2\text{O}$, >98%) and calcium chloride dihydrate ($\text{CaCl}_2 \cdot 2\text{H}_2\text{O}$, $\geq 99\%$) were

acquired from Riedel-de-Haën (North Caroline, USA); and iron(III) chloride hexahydrate ($\text{FeCl}_3 \cdot 6\text{H}_2\text{O}$, $\geq 97\%$) was purchased from PRS Panreac (Barcelona, Spain). The medium is aerated for 60 minutes and inoculated with *R. subcapitata* stored from a previous culture and maintained for 7 days, at uniform light (6000 lux for bottom illumination), 16 : 8 h light/dark, at $20 \pm 2^\circ\text{C}$ and an air pump system with continuous magnetic agitation (**Figure 5**). After 7 days of incubation, 250 mL of the microalgae culture was used for the next culture. The remainder of the microalgae culture was transferred to 50 mL falcon tubes and centrifuged at 3000 rotations per minute (rpm) for 10 minutes. The supernatant was discarded and the algae pellet was reconstituted in 2 mL of MHRW medium. The optical density (OD) of algae suspension was measured at a wavelength of 440 nm and adjusted 0.6 and 0.8. The algae suspension was kept at 4°C and used as food for the daphnia.



Figure 5 | Algae culture medium, in magnetic agitation, with 2 Teflon tubes: 1-tube for airflow out, 2-tube with filtered air supply with a $0.22 \mu\text{m}$ filter that connects to an air pump system.

3.2.4 | Experimental design

Each experimental unit consisted of a glass flask with 200 mL of MHRW medium with 15 daphnia of 3rd generation (neonates less than 24h old) and 5 replicates per each concentration and control (**Figure 6**). Organisms were exposed to environmental and sublethal concentrations of MDMA racemate and each enantiomer for 8 days, to follow the ontogenetic period, i.e., initial life stages and first reproductive events. The organisms were incubated in a bioterium at $20 \pm 2^\circ\text{C}$ and 16 : 8 h (light/dark).

The MDMA racemate assay was performed using three concentration levels, 0.1, 1 and 10 µg/L. The enantiomers assay was performed using two concentration levels, 0.1 and 1 µg/L. The culture medium was renewed and organisms fed with a *R. subcapitata* ratio of 3.0×10^5 (neonates and juveniles) or 6.0×10^5 (adults) cells/mL at every 48-hour intervals.

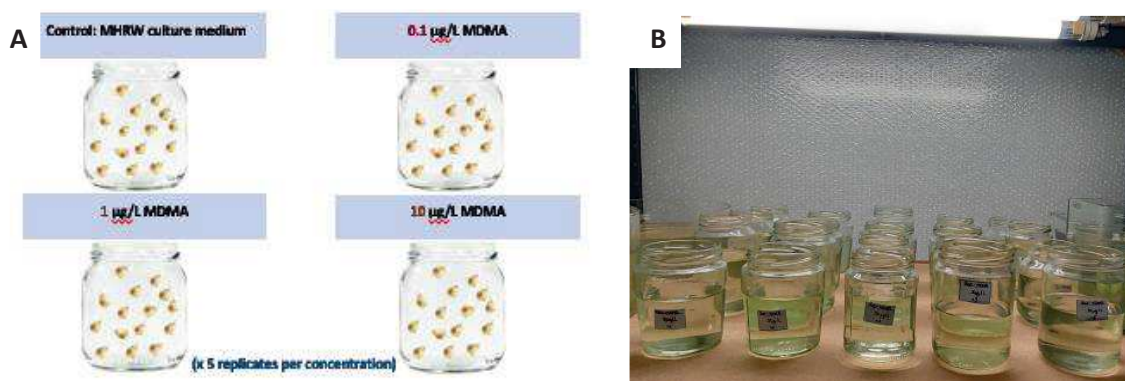


Figure 6 (A) Schematic representation of the toxicity assay with a control group and three different concentrations of (*R,S*)-MDMA, 5 replicates of each group. (B) Photo of the toxicity assay with (*R,S*)-MDMA, showing the arrangement of flasks with 200mL of MRHW medium each.

The ecotoxicity assay was designed to include different endpoints as morphophysiological parameters (body size, heart area and size, and heart rate), biochemical parameters (determination of oxidative stress and enzymatic activity) reproductive parameters (number of daphnia with eggs and number of eggs per daphnia) and swimming behaviour (**Figure 7**). On days 3 and 8, three random daphnia per replicate were collected and used for the determination of morphophysiological parameters. On day 5, swimming behavioural was determined using six random daphnia per replicate. On day 8, three random daphnia per replicate were collected for determination of the reproductive parameters. At the end of all determinations (day 8), organisms from each replica were collected into a 2 mL eppendorf. The culture medium was removed and organisms washed with PBS to completely remove the culture medium, reconstituted with 250 µL of cold PBS and stored at -80°C until biochemical analysis.

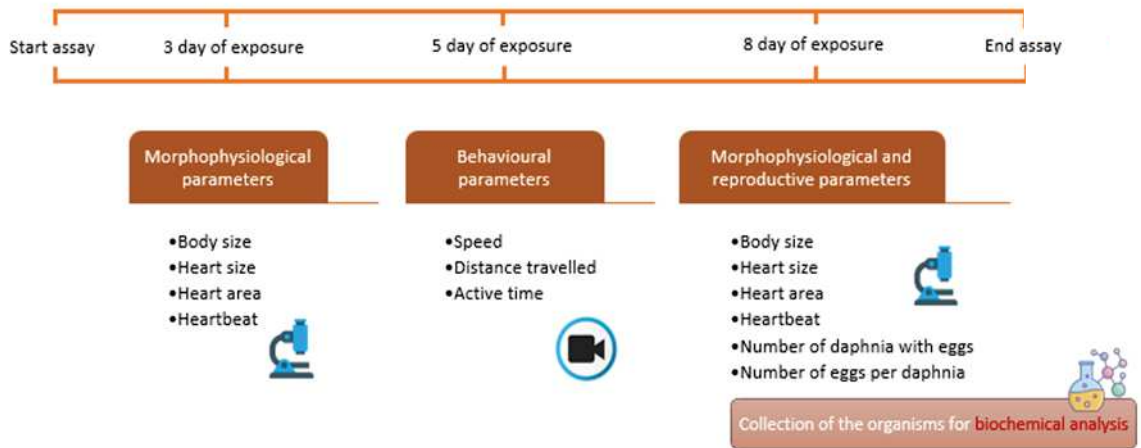


Figure 7|Schematic representation of the experimental design.

3.2.5| Morphophysiological parameters

The determination of morphophysiological parameters was performed on days 3 and 8. For that, 3 random daphnia per replicate were collected. Each organism was transferred to a slide with 2/3 drops of culture medium and placed under a microscope coupled to a digital camera (Canon PowerShot G9, **Figure 8**). The organism was photographed and video recorded for approximately 1 minute and 5 seconds, using the 5x objective and medium zoom. After that, the organisms were placed back into the corresponding replica flask and the images and videos were analysed in specific software.



Figure 8|Optical microscope coupled to the digital camera to video recording to assess morphophysiological parameters using specific software.

For body size and heart area and size, images were analyzed using the software Digimazer® Ver. 5.3.4 (**Figure 9**).

For heart rate determination (beats per minute, bpm), videos length were adjusted to 1 minute and a speed of 0.25x the original video, using the windows video editor. The number of heartbeats per daphnia was determined using the Counter UX: Click counter application.

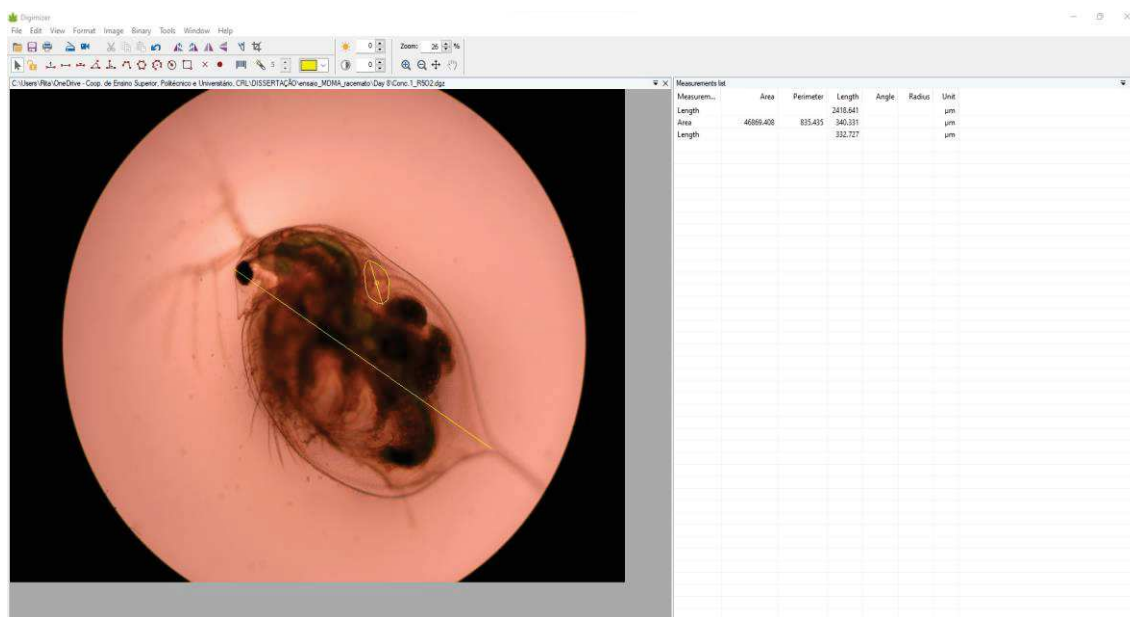


Figure 9 | Digimazer program layout with body size, heart area and size measurements.

3.2.6 | Swimming behaviour

The parameters (swimming speed, total distance travelled and active time) were determined on day 5 by recording daphnia in a 6-well plates. The wells were filled with 5 mL of melted 1% agarose gel and the plates were placed in the refrigerator at 4°C. After the gel solidified, a central portion of the agarose gel was cut, creating a circular area that served as a barrier to the swimming of organisms and improved the optics at the edge of the well.

Each replica corresponded to one 6-well plate. Thus, 5 mL of MHRW culture media were transferred to each well and 6 random daphnids per replicate were individually transferred to each well. The plates were placed on top of a laptop screen with a white background and the organisms were recorded for 1 minute and 30 seconds using a digital camera

(Canon Legria HF R506, with a resolution of 30 frames/s) mounted on a perpendicular position, as shown in **Figure 10**. At the end, the organisms were transferred to the respective flask.



Figure 10 | Equipment used for video record of daphnia swimming behaviour.

The videos were edited using the DaVinci Resolve 17 program, to obtain the videos of each isolated plate and with 1 minute of duration each and then processed in the program The Real Fish Tracker (Ver. 0.4.0) to analyse the following parameters: swimming speed, total distance travelled and active time. **Figure 11** shows the layout of the software's used for video processing.

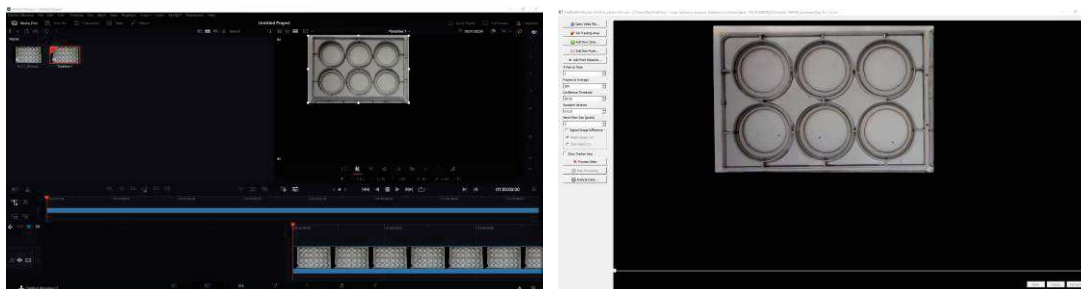


Figure 11 | DaVinci Resolve 17 (in the left) and The Real Fish Tracker (0.4.0) (in the right) programs used for swimming behavioural determinations.

3.2.7| Reproduction parameters

The reproductive parameters such as number of daphnia with eggs and number of eggs per daphnia were obtained on day 8 using the same images from morphophysiological parameters.

3.2.8| Biochemical parameters

Organisms were collected at the end of the assays and stored in a phosphate buffer solution (PBS, pH 7.6), composed of 0.800 g NaCl, 0.020 g KCl, 0.144 g Na₂HPO₄ and 0.024 g KH₂PO₄ in a 100 mL of UPW. Before biochemical analysis, daphnid tissue was homogenized via ultrasonication, centrifuged at 13 000 g for 20 min at 4 °C and the supernatant was immediately collected for the determinations.

3.2.8.1| Protein quantification

Protein was measured using Bradfords assay. This is a colorimetric assay where a dye is added that binds directly to the proteins.

For this assay, BSA calibration curve was constructed using 7 standards and a blank according to the Annex III. Each sample was analysed in duplicate and using 2 µL of sample for protein quantification, 98 µL of PBS and 100 µL of Bradford reagent and incubated for 5 min at RT transferred into 96 well microplate and the absorbance read at 595 nm using a microplate reader.

3.2.8.2| Acetylcholinesterase activity (AChE)

AChE activity was calculated with an assay based on an improved Ellman method. The assay uses DTNB to quantify the thiocholine produced from the hydrolysis of ATCI by AChE. Thiocholine produced forms a yellow colour with DTNB, generating 5-thio-2-nitrobenzoic acid (TNB).

A duplicate was performed for each sample and blank. Samples for AChE activity were prepared in 1.5 mL Eppendorf with 20 µL of sample, 120 µL of 0.5 mM DNTB and 60 µL of 20 mM ATCI and transferred into 96 well microplate. After incubation for 5 min at RT, the absorbance was read at 412 nm for 3 min at 25 °C. The AChE concentration was calculated following the next formula:

$$\varepsilon = \frac{A}{c \times l}, \text{ were}$$

TNB extinction coefficient ($\epsilon_{412 \text{ nm}}$) of $14.1 \times 10^3 \text{ M}^{-1}\text{cm}^{-1}$ ($\text{L mol}^{-1}\text{cm}^{-1}$; $14.1 \text{ mmol}^{-1}\text{mL cm}^{-1}$), optical path (l) of 0.8 cm, absorbance of sample (A) and molar concentration (c). AChE concentration (mol/mL) was multiplied for dilution factor and divided for BSA concentration (mg/mL protein), the results were expressed as $\text{mmol TNB/mg protein}$.

3.2.8.3| Reactive oxygen species (ROS)

ROS assay uses a fluorescent probe (H_2DCFDA), a cell permeant reagent fluorogenic dye that can freely cross the membrane and measures hydroxyl, peroxy and other ROS activity in the cell. After entering the cell, it is hydrolysed by intracellular esterase to form a non-fluorescent compound, DCFH. In the presence of ROS, DCFH is oxidized to DCF which is a strong green, fluorescent substance (Pourahmad et al. 2003).

Standards solution and blank were prepared in 1.5 mL Eppendorf's according with the Annex III and incubated for 5 min at RT. Samples for ROS determination were prepared in 1.5 mL Eppendorf's with 10 μL of sample, 8.3 μL of 21 mM H_2DCFDA , and 110 μL of PBS and incubated for 5 min at RT in duplicate. The fluorescence of DCF was read at 25 °C with an excitation λ of 485 nm and an emission λ of 528 nm. The intensity is proportional to the level of intracellular ROS, and the results were expressed as $\mu\text{mol DCF/mg protein}$.

3.2.8.4| Catalase activity (CAT)

The enzymatic activity of CAT was determined with a spectrophotometric method at 415 nm and 25 °C. The standards of CAT and samples were incubated with $\text{H}_2\text{O}_2/\text{PBS}$ at 37 °C for 1 min, and the enzymatic reaction was stopped by the addition of metatartaric acid (AMT). After incubating at RT for 5 min, the residual H_2O_2 reacts with AMT to generate a yellowish complex (molybdate/ H_2O_2 complex). CAT activity is directly proportional to the rate of dissociation of H_2O_2 , and the results were expressed as U CAT/mg protein. The assay was performed in duplicate according to the Annex III. Then, 100 (μL) of each sample was transferred to a 96-well microplate and the absorbance was read.

3.2.8.5| Thiobarbituric Acid Reactive Substances (TBARS)

The MDA level was determined via the TBARS colorimetric method by measuring the absorbance of MDA and TBARS (Ghani et al. 2017; Tsikas 2017). TBARS and TBA can react under high temperatures and acid conditions to form a pink compound, the MDA-TBA adduct. The results are expressed as $\mu\text{mol MDA/mg protein}$.

Standards and blank were prepared and incubated for 15 min at RT according to the Annex III. Samples for MDA determination were prepared according to **Table 3** and incubated for 2 hours at 60 °C, then cooled for 15 minutes on ice and then, 20 % Sodium Dodecyl Sulphate (SDS) pre-heated was added. The assay was performed in duplicate and 200 μL of each sample was transferred to a 96 well microplate and the absorbance read at 530 nm.

Table 3 | Preparation of samples for MDA determination.

Sample (μL)	H ₂ O UP (μL)	50 mM PBS (μL)	1 mM BHT (μL)	1.3% TBA/0.3% NAOH (μL)	50 % TCA (μL)	20% SDS* (μL)
10	70	50	10	75	50	10

*Incubate for 2 hours at 60°C and cool for 15 min on ice. After added 20% SDS (pre-heated at 68°C).

3.3 | Statistical Analysis

The statistical analysis of the data was carried out using software Jamovi version 2.2.2. General linear model (one-way ANOVA) followed by Dunnett contrasts to investigate the significant effects of racemate on morphophysiological, swimming behaviour and biochemical parameters. Reproductive parameters were analysed as count data using generalized linear model by negative binominal model followed by Dunnett contrasts. The differences were considered statistically significant at $p < 0.05$. Data from the enantiomer experiment were analysed with general linear models (two-way ANOVA) to assess significant effects of MDMA concentrations and its enantiomeric forms on morphophysiological, behavioural, and biochemical parameters. Significant differences relative to the control were analysed with Dunnett contrasts. Reproductive endpoints were analysed with generalised linear models (negative binomial GLM), following analogous approaches to the two-way ANOVA.

4| Results and Discussion

4.1| Multimilligram enantioresolution of MDMA

4.1.1| Injection volume optimization

The enantioseparation of (*R,S*)-MDMA was performed in a semi-preparative amylose 3,5-dimethylphenylcarbamate column (500 Å, 7 µm, 20%, w/w; 20 x 0.7 cm internal diameter) following the previously established conditions by Gonçalves et al. (2019). The mobile phase consisted of *n*-Hex with 0.1% DEA and EtOH with 0.1% DEA in a ratio of 80:20 v/v, a flow-rate of 1.5 mL/ min and the detection wavelength of 210 nm, (**Figure 12**).

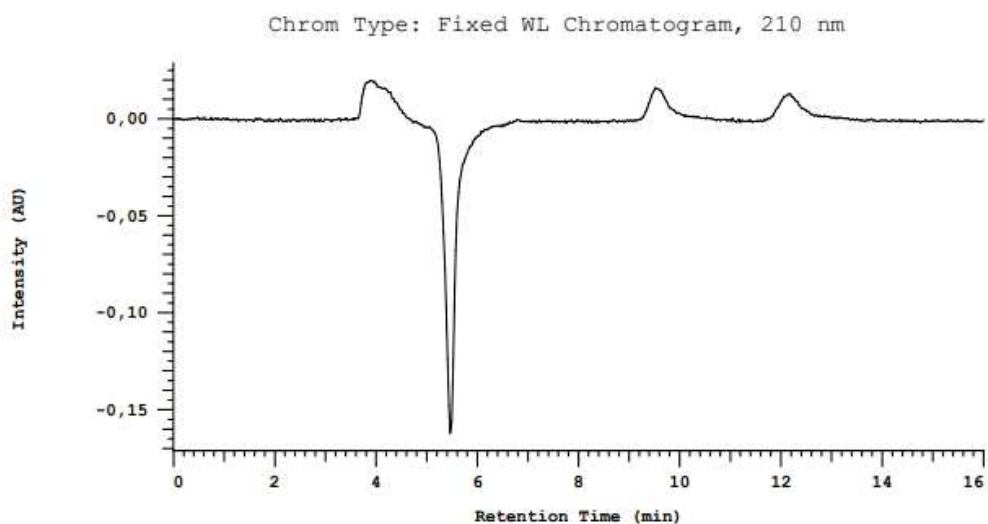


Figure 12|Chromatogram showing the separation of (*R,S*)-MDMA enantiomers [*R*(-)-MDMA and *S*(+)-MDMA] in semi-preparative amylose 3,5-dimethylphenylcarbamate column by LC-DAD under normal phase. Mobile phase: *n*-Hex (0.1% DEA) and EtOH (0.1% DEA), 80:20 v/v; flow-rate: 1.5 mL/min; detector:210 nm; injection volume: 5 µL. Standard solution at 1 mg/mL (EtOH).

The injection volume was optimized for the enantiomeric separation of (*R,S*)-MDMA using a stock solution of 30 mg/mL MDMA in EtOH. The strategy consisted of studying different injection volumes considering the column overload capacity, to make the process as profitable as possible in terms of purity, yield and number of injections while maintaining a good resolution. **Figure 13** shows the chromatograms with 5, 10, 15 and 20 µL of injection. Once a good separation of the fractions with the highest volume was obtained, the optimized conditions for enantioseparation was established with injection volume of 20 µL at 30 mg/mL.

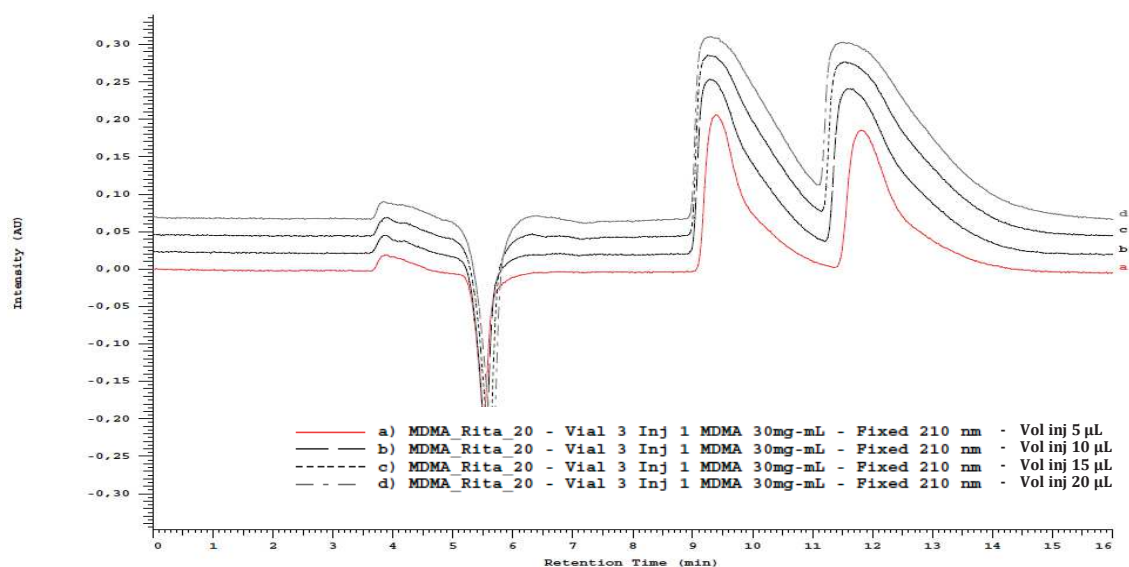


Figure 13 Chromatogram showing the injection volume optimization for the enantioseparation of (*R,S*)-MDMA in semi-preparative amylose 3,5-dimethylphenylcarbamate column by LC-DAD under normal elution mode. Mobile phase: *n*-Hex (0.1% DEA) and EtOH (0.1% DEA), 80:20 v/v; flowrate: 1.5mL/min; detector: 210 nm. Standard solution at 30 mg/mL (EtOH) and injection volume Line a) 5 µL; line b) 10 µL; line c) 15 µL; and line d) 20 µL.

4.1.2| Enantioseparation

The elution order of each enantiomer, under these conditions, was previously determined by Gonçalves et al. (2019), showing a longer retention time of the *S*(+)-enantiomer compared to the *R*(-)-enantiomer (**Figure 14**). Thus, the *R*(-)-MDMA enantiomer was first eluted and collected from 9 to 11 minutes and *S*(+)-MDMA was collected from 11.5 to 15 minutes. An intermediate fraction was collected (from 11 to 11.5 minutes), concentrated and re-injected (injection volumes of 100 µL) to avoid the contamination of previous collected fractions and assure high purity and yield (**Figure 15**).

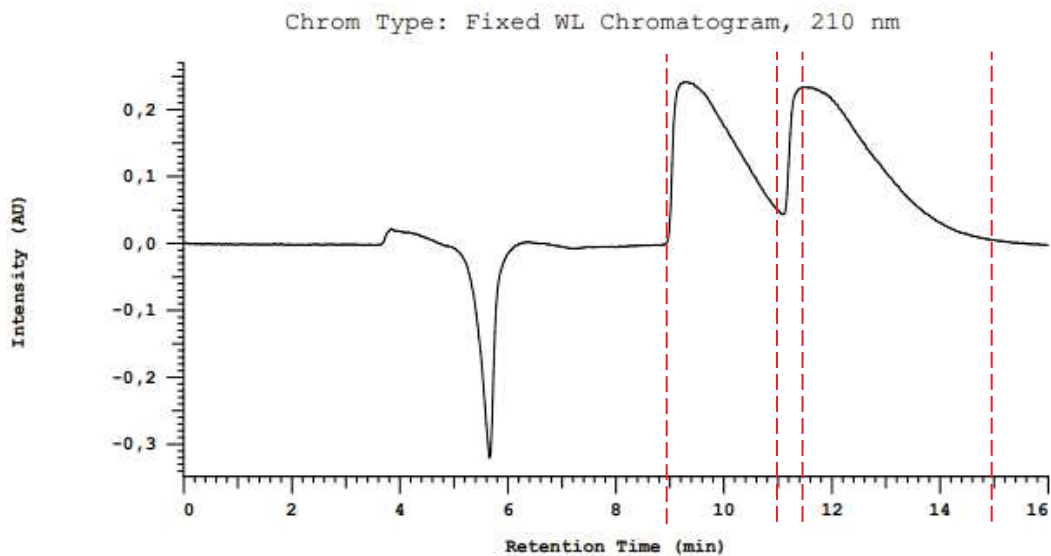


Figure 14 Chromatogram showing the separation of MDMA enantiomers [*R*(-)-MDMA and *S*(+)-MDMA] in the semi-preparative amylose 3,5-dimethylphenylcarbamate column by LC-DAD under normal elution mode. Mobile phase: *n*-Hex (0.1% DEA) and EtOH (0.1% DEA), 80:20 v/v; flowrate: 1.5 mL/min; detector: 210 nm; injection volume: 20 μ L. Standard solution at 30 mg/mL (EtOH). The red dotted line corresponds to the cut-off time, that is, the time when each enantiomeric fraction was collected in the respective flask. The fraction corresponding to *R*(-)-MDMA was collected from 9 minutes to 11 minutes, the intermediate fraction was collected from 11 minutes to 11.5 minutes and the fraction corresponding to *S*(+)-MDMA was collected from 11.5 to 15 minutes.

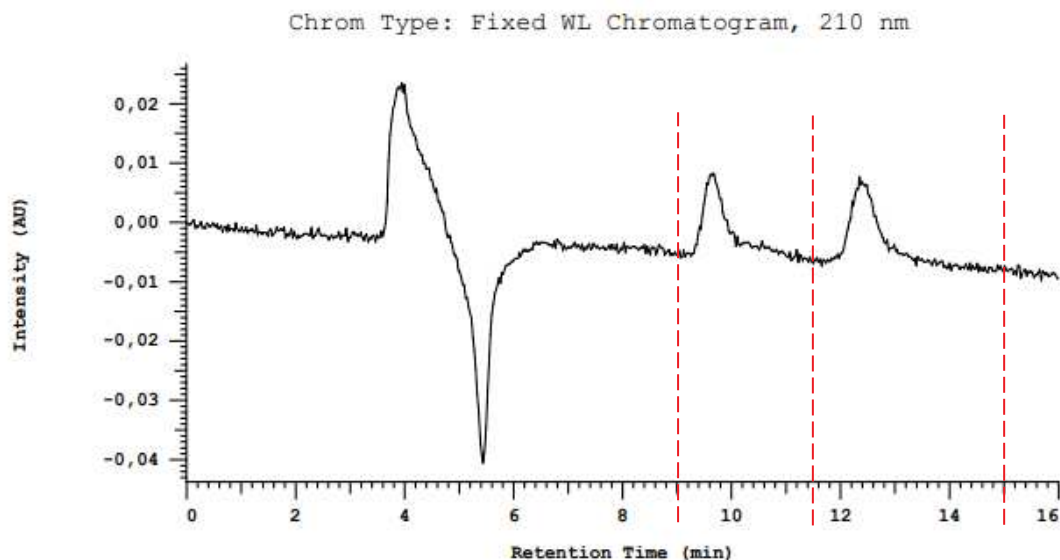


Figure 15 Chromatogram showing the separation of MDMA enantiomers [*R*(-)-MDMA and *S*(+)-MDMA] in the semi-preparative amylose 3,5-dimethylphenylcarbamate column by LC-DAD under normal elution mode. Mobile phase: *n*-Hex (0.1% DEA) and EtOH (0.1% DEA), 80:20 v/v; flowrate: 1.5mL/min; detector: 210 nm; injection volume: 100 μ L of intermediate fraction. The red dotted line corresponds to the cut-off time, that is, the time when each enantiomeric fraction was collected in the respective flask. The fraction corresponding to *R*(-)-MDMA was collected from 9 minutes to 11.5 minutes and the fraction corresponding to *S*(+)-MDMA was collected from 11.5 minutes to 15 minutes.

4.1.3| Enantiomeric purity analysis

Enantiomeric purity was evaluated using the semipreparative amylose 3,5-dimethylphenylcarbamate column and in the same conditions used for MDMA enantioseparation but with an injection volume of 100 μ L each. As can be seen in the chromatogram and spectra present in **Figure 16**, the e.r. of the first fraction corresponding to the *R*(-)-MDMA enantiomer – spectrum a) was approximately 99.9%. The second fraction (spectrum b) corresponding to the *S*(+)-MDMA enantiomer was obtained with an e.r. of 97%.

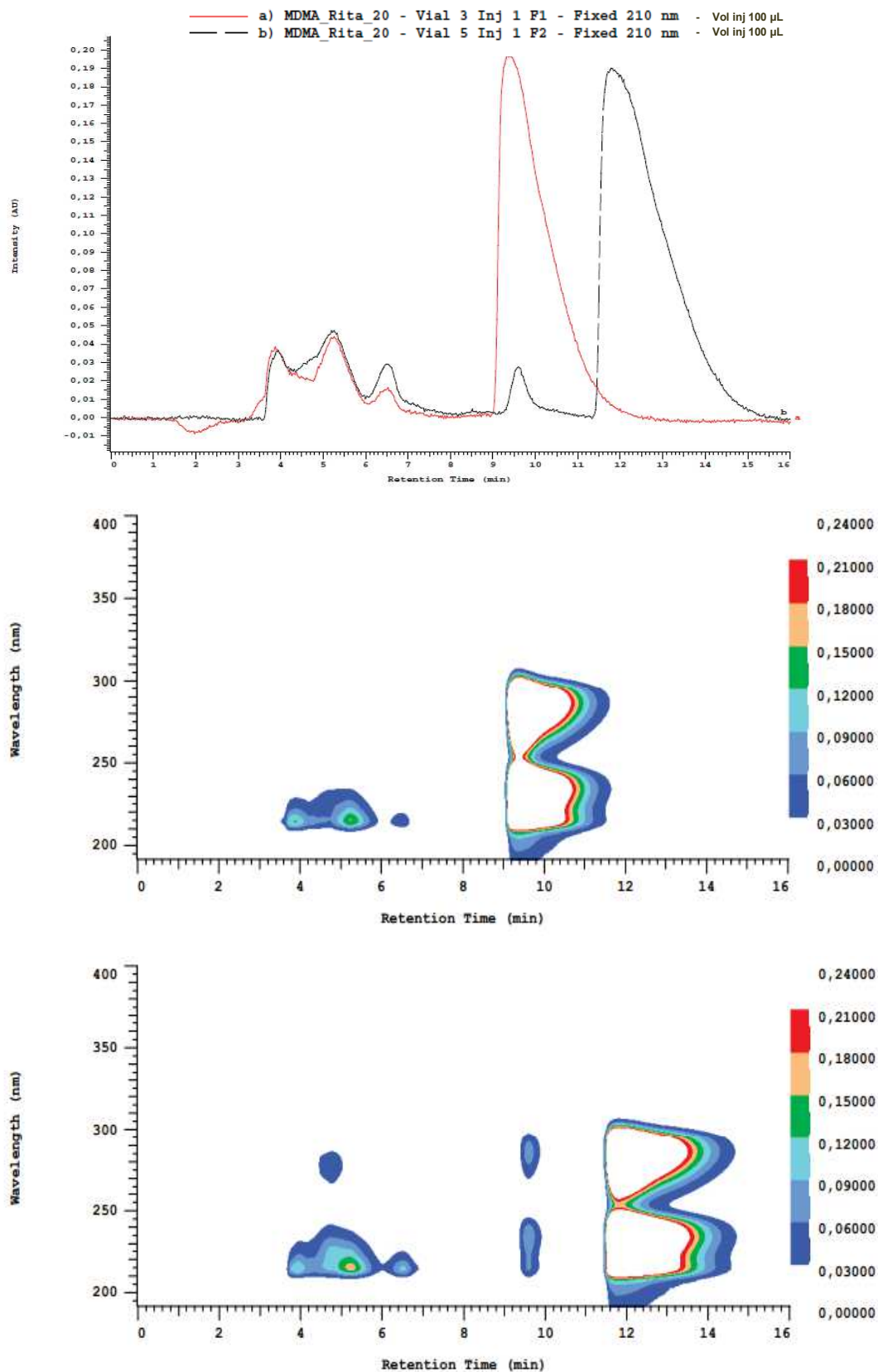


Figure 16 Chromatogram and absorption spectra (absorbance scale: 0.240) showing *R(-)*-MDMA and *S(+)*-MDMA fraction analysis in the semi-preparative amylose 3,5-dimethylphenylcarbamate column by LC-DAD under normal elution mode. Mobile phase: *n*-Hex (0.1% DEA) and EtOH (0.1% DEA), 80:20 v/v; flow-rate: 1.5 mL/min; detector: 210 nm; injection volume: 100 μ L. Legend: Chromatogram representing *R(-)*-MDMA fraction in line a/red (absorption spectra above) and *S(+)*-MDMA fraction in line b/black (absorption spectra below).

4.1.4| Quantification/recovery of enantiomers

For quantification of the enantiomers recovered from the semi-preparative enantioresolution, two different analytical columns and several chromatographic conditions were tested. First, the Lux® 3 μm Cellulose-4 (Cellulose tris(4-chloro-3-methylphenylcarbamate), 150 x 4.6 mm), was tested in normal and reversed elution mode (Table 4), but enantioseparation was not achieved in any tested conditions.

Table 4|Chromatographic conditions optimization for the recovery determination of MDMA enantiomers.

Equipment	Mobile phase	Proportion (v/v)	Injection volume (μl)	Flow-rate (mL/min)	Column	λ (nm)	K	α	R
HPLC-DAD	n-Hexan (0.1% DEA)	80:20	10	0.500	Celulose-4	295	-	-	-
	: EtOH (0.1% DEA)	90:10	5	1.000	Celulose-4		-	-	-
	UPW + Ammonium	90:10	10		Celulose-4		-	-	-
	Acetate : Isopropanol	80:20	10		Celulose-4		-	-	-
	Ammonium Acetate: EtOH	90:10	10	0.500	Celulose-4		-	-	-
	Methanol : Ammonium Bicarbonate (0.1% DEA)	50:50	15		Celulose-4		-	-	-
		70:30	15		Celulose-4		-	-	-
LC-UV/Vis LC-FD	EtOH : UPW (0.1% DEA)	65:35	10	0.1	i-Amylose 3	210	2.9; 3.6	1.2	1.9
		70:30	10		i-Amylose 3		2.0; 2.5	1.2	1.5

Enantioseparation was achieved with Lux® 3 μm i-Amylose-3 column (LC Column 150 x 2.0mm) with a mixture of EtOH and UPW with 0.1% DEA (65:35, v/v) as mobile phase. However, to achieve the best chromatographic performance (reduce retention time while maintaining enantioseparation and good resolution), the mobile phase was tested at different proportions (v/v) of 65:35 and 70:30. Increasing EtOH decreases retention time (Figure 17). The optimized conditions were established with the Lux® 3 μm i-Amylose-3 column) in reversed elution mode with a mixture of EtOH and UPW with 0.1% DEA (70:30, v/v) as mobile phase, flow-rate of 0.1 mL/min, a wavelength of 210 nm and injection volume of 10 μL . Enantioseselctive ($\alpha=1.2$) and adequate resolution ($R=1.5$) were achieved with the retention times of 16.0 and 18.5 minutes for *R*(-)-MDMA and *S*(+)-MDMA, respectively.

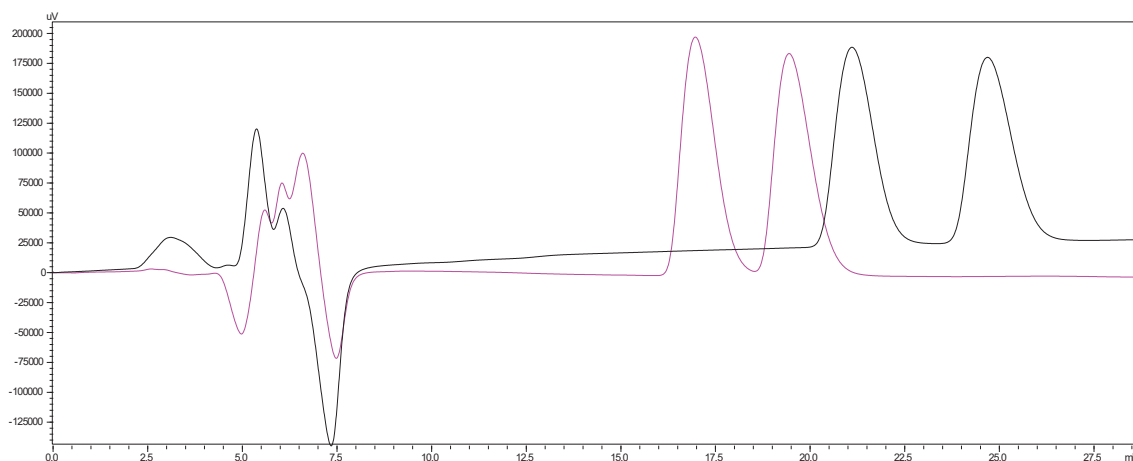


Figure 17 | Chromatogram showing the separation of MDMA enantiomers in the analytical column (Lux® 3µm i-Amylose-3 column) in reversed elution mode. Mobile phase: EtOH and UPW with 0.1% DEA; flowrate: 0.1mL/min; detector:210 nm; injection volume: 10 µL. Standard solution at 100 µg/mL (EtOH). Legend: Black line - EtOH and UPW with 0.1% DEA (65:35, v/v), and Pink line - EtOH and UPW with 0.1% DEA (70:30, v/v).

An analytical method was validated with the propose to quantify the enantiomers collected from the semi-preparative enantioresolution. The calibration curves were found to be linear in the range of 5.0 to 50 µg/mL with R^2 greater than 0.9996 for *R*(-)-enantiomer; and a range of 5.0 to 75 µg/mL with R^2 equal to 1.0000 for *S*(+)-enantiomer (Table 5).

Table 5 | Results of MDMA enantiomers recovery obtained by semi-preparative chromatography.

<i>Enantiomer</i>	<i>Range (µg/mL)</i>	<i>Linear Equation</i>	<i>Correlation level (R²)</i>	<i>Recovery concentration (µg/mL)</i>	<i>Recovery (%)</i>
<i>R</i> (-)-MDMA	5.0 – 50.0	Y=229471x+158183	0.9996	6095.79	40.64
<i>S</i> (+)-MDMA	5.0 – 75.0	Y=224541.08x+277228.35	1.0000	293.17	1.95

Aproximately a total of 50 injection in the semi-preparative column were done for enantioseparation of the stock solution of MDMA. If a 100% recovery was obtained, it would be expected to obtain 15 mg of each enantiomer. Calculating and multiplying by the dilution factor, an *R*(-)-enantiomer concentration of 6095.79 µg/mL and 293.17 µg/mL of *S*(+)-MDMA was obtained. The recovery percentage was 40.6% for *R*(-)-MDMA and 2.0% for *S*(+)-MDMA (6.09 mg of *R*(-)-MDMA and 0.3 mg of *S*(+)-MDMA).

During the crystallization process to obtain the hydrochloride leads to the appearance of an oil that may justify the loss of a large amount of the enantiomers and the low recovery obtained namely for the *S*(+)-enantiomer.

4.2| Ecotoxicity assays

A sub-chronic exposure was performed starting from day 0 to day 8 in concentrations selected to include reported environmental relevant levels: 0.1 and 1.0 µg/L and a worst-case scenario at 10 µg/L for (*R,S*)-MDMA, and 0.1 and 1.0 µg/L for each enantiomer to investigate possible enantioselective effects on *D. magna*.

4.2.1| Morphophysiological parameters

Some studies have shown that morphophysiological endpoints can be used as indicators of water contaminants toxicity due to their sensitivity at sublethal concentrations (Gustinasari et al. 2021; Li et al. 2021; Pérez-Pereira et al. 2022; Szabelak and Bownik 2021). Exposure of aquatic organism to PAS has been shown to interfere with the development of aquatic organisms in an enantioselective way. For instance, an increase in malformations (e.g., pericardium oedema, eye area) was observed during zebrafish embryo development exposed to (*R*)-venlafaxine (Ribeiro et al. 2022).

Both racemate and enantiomers negatively affected morphophysiological parameters at different stages of daphnia life cycle. Different effects were observed in the organism exposed to the racemate. A decrease in body size in juveniles was observed at 1 and 10 µg/L whereas an increase in body growth was found in adult organisms at the highest concentration (**Figure 18**). An enantioselective effect was observed in body size with *S*(+)-MDMA showing a significant decrease at the highest concentration whereas *R*(-)-MDMA not interfered with body growth for either juveniles and adults (**Figure 19, Table 6**). Similar results were observed in our previous study, in organisms exposed to AMP racemate and *S*(+)-AMP (data not published yet).

Heart development also showed to be affected by the racemate but only in the juveniles. A significant reduction in heart area and size was noted. Heart area and size and heart rate were not affected in adults (**Figure 18, Table 6**). This result is of concern as 0.1 µg/L is among environmental concentrations. No enantioselective effects or changes were found in heart area and size and heart rate at both day 3 and day 8 (**Figure 19, Table 6**). These

results show that MDMA can interfere with morphophysiological parameters during different stages of daphnia development and that the effect can be enantioselective.

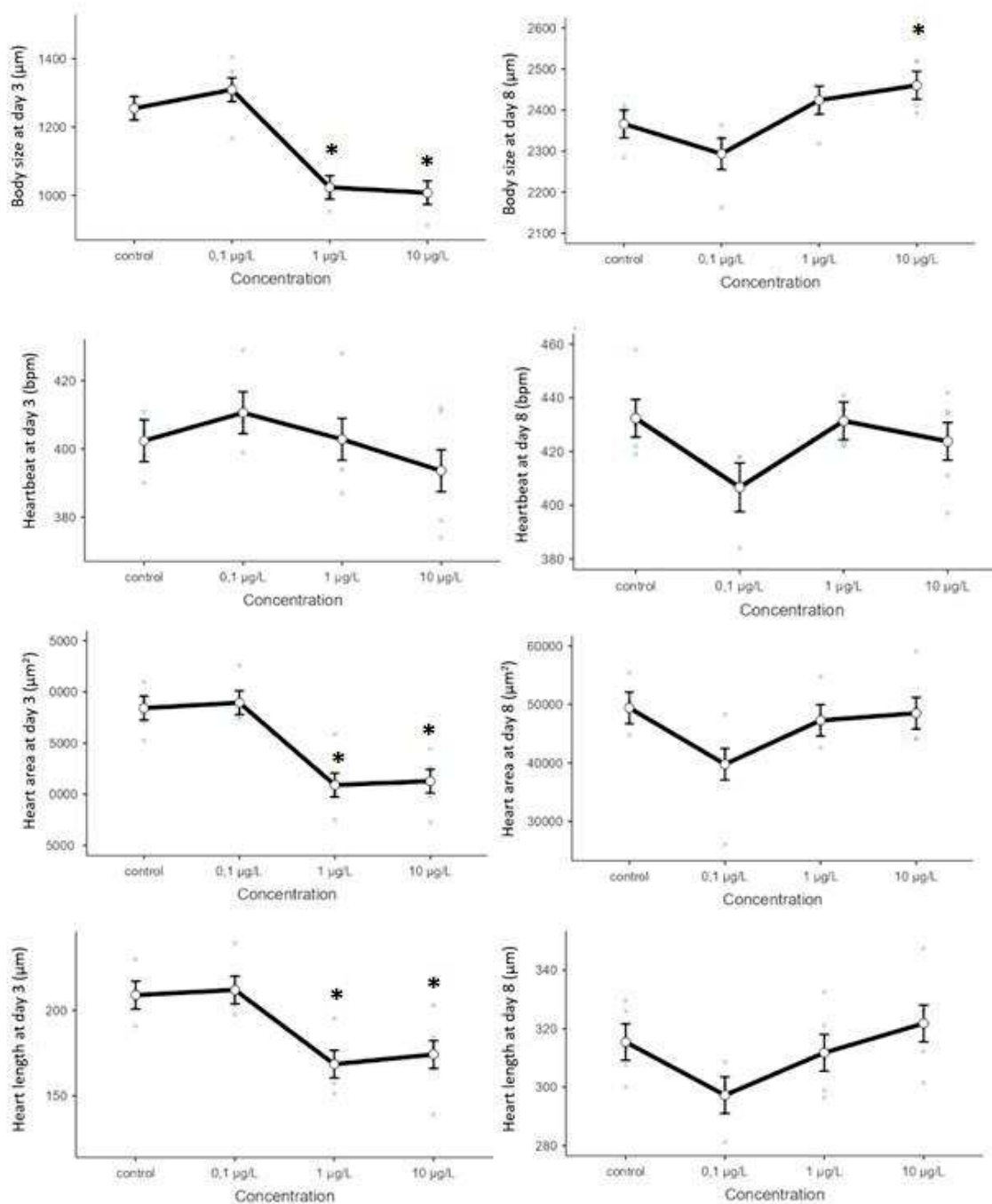


Figure 18 Morphophysiological effects of racemic MDMA determined at day 3 (in the left panel) and day 8 (in the right panel). Note: Asterisks (*) represent significant differences relatively to the control.

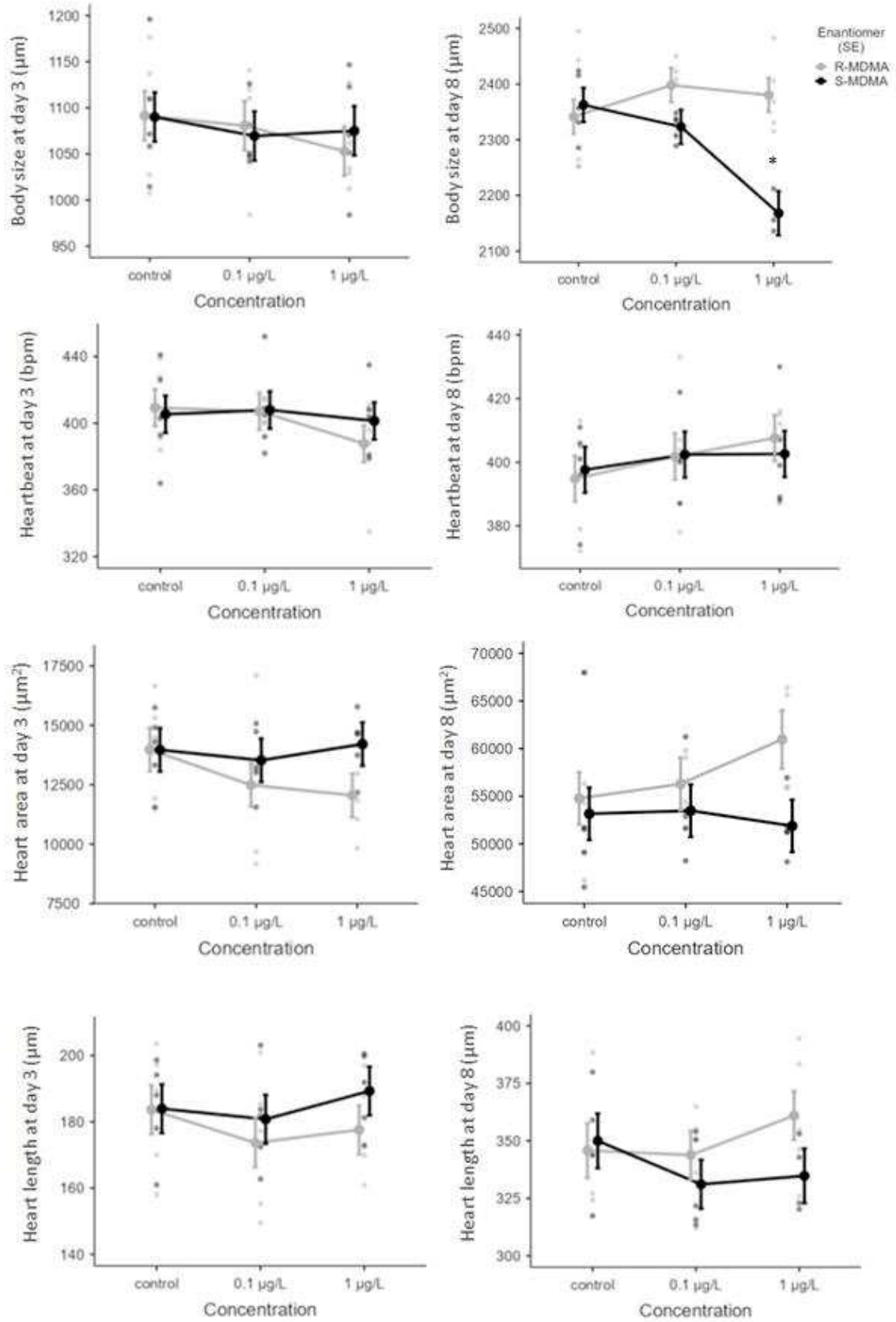


Figure 19 Morphophysiological effects of MDMA enantiomers determined at day 3 (in the left panel) and day 8 (in the right panel). Note: Asterisks (*) represent significant differences relatively to the control.

Table 6 | Statistical analysis of morphophysiological effects of MDMA racemate and enantiomers on *D. magna*, determined at day 3 and 8. Significant effects ($p < 0.05$) in bold.

Variable	Source of variation	Day 3		Day 8	
		F	<i>p</i>	F	<i>p</i>
Body size (μm)	<i>rac</i>	20.4	<0.001	4.05	0.012
	Enantiomer	0.0212	0.885	5.72	0.003
	Concentration	0.5061	0.609	1.50	0.034
	Interaction	0.2036	0.817	3.04	0.007
Heart size (μm)	<i>rac</i>	7.87	0.002	2.76	0.076
	Enantiomer	1.129	0.298	1.587	0.222
	Concentration	0.508	0.608	0.607	0.554
	Interaction	0.303	0.741	0.867	0.435
Heart area (μm^2)	<i>rac</i>	14.3	<0.001	2.66	0.083
	Enantiomer	2.03	0.167	3.88	0.061
	Concentration	0.661	0.525	0.384	0.688
	Interaction	0.707	0.503	0.992	0.386
Heart rate (bpm)	<i>rac</i>	1.29	0.313	2.02	0.158
	Enantiomer	0.146	0.706	0.00813	0.929
	Concentration	0.899	0.420	0.781	0.469
	Interaction	0.335	0.718	0.154	0.858

4.2.2| Swimming behaviour

Behavioural responses are also important indicators of toxicity. Changes in swimming behaviour of aquatic organisms have been reported for several PAS, such as BE, COC, MDMA (De Felice et al. 2019; Parolini et al. 2018; Stewart et al. 2012).

In our study, a significant increase ($p < 0.001$) in swimming speed was observed in the organisms exposed to all concentrations of (*R,S*)-MDMA whereas no changes were observed for the enantiomers (**Figure 20, Table 7**). A significant increase in total distance travelled at 0.1 and 1 $\mu\text{g/L}$ of the racemate but a significant decrease in distance travelled at 10 $\mu\text{g/L}$ was observed (**Figure 20, Table 7**). These results are in agreement with those obtained in the study developed by De Felice et al. (2019) for COC, which show that exposure to higher concentrations of the substance leads to a decrease in the distance travelled by daphnia, while exposure to lower concentrations leads to an increase in the distance travelled. A significant decrease was also observed for both enantiomers at the two concentrations and no enantioselectivity was observed (**Figure 20, Table 7**). Similar results were found for organisms exposed to AMP racemate and its enantiomers (data not

published yet). A significant decrease of active time was also observed for the racemate at all concentrations but no changes were observed for the enantiomers.

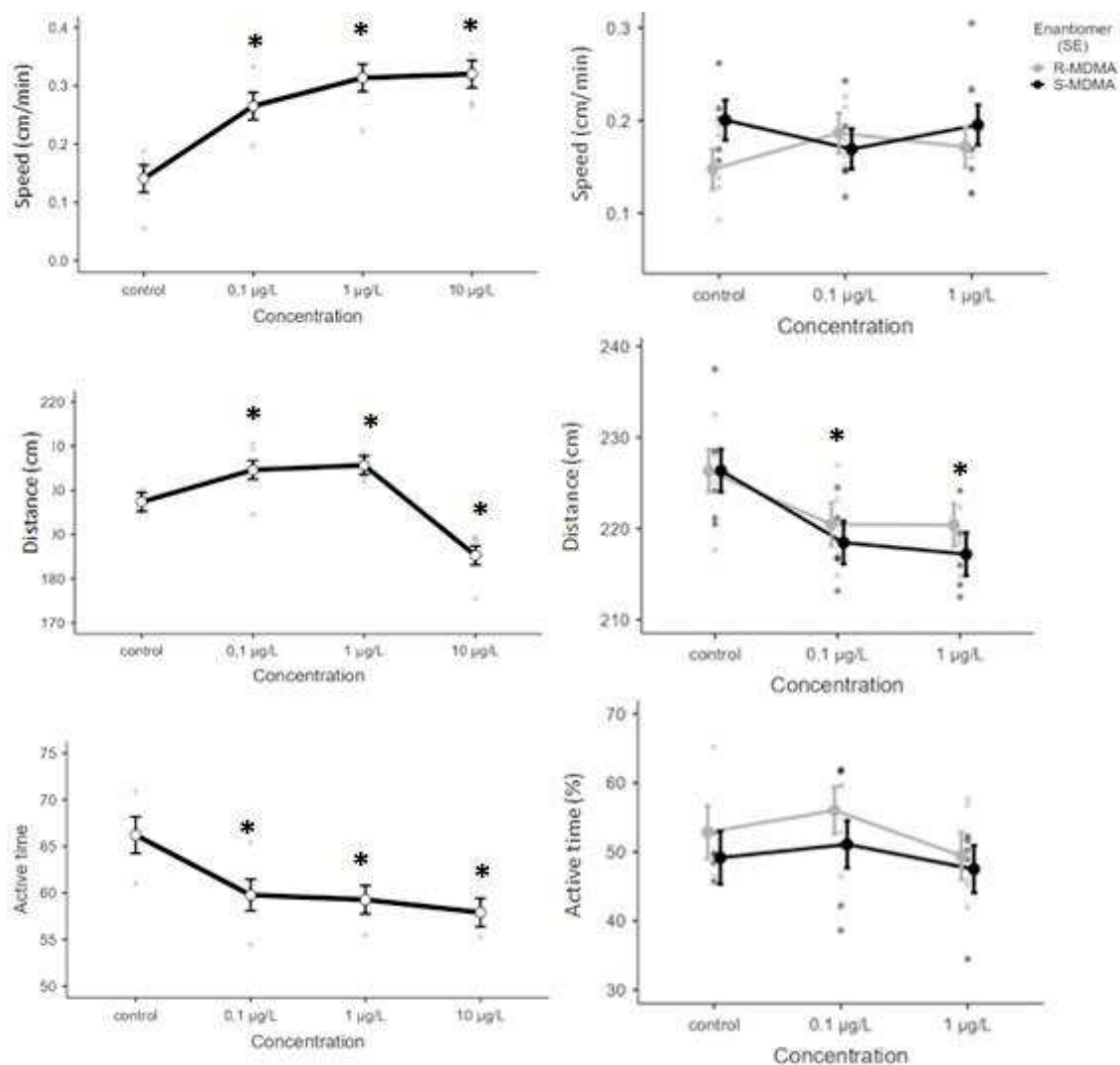


Figure 20 | Swimming behaviour effects of MDMA racemate (in the left panel) and enantiomers (in the right panel), determined at day 5. Note: Asterisks (*) represent significant differences relatively to the control.

Table 7|Statistical analysis of swimming behaviour effects of MDMA racemate and enantiomers on *D. magna*, determined at day 5. Significant effects ($p < 0.05$) in bold.

Variable	Source of variation	F	p
Speed (cm/min)	<i>rac</i>	12.5	<0.001
	Enantiomer	1.2534	0.274
	Concentration	0.0949	0.910
	Interaction	1.33	0.282
Total Distance travelled (cm)	<i>rac</i>	19.5	<0.001
	Enantiomer	0.804	0.379
	Concentration	6.306	0.006
	Interaction	0.236	0.791
Active time (%)	<i>rac</i>	1.29	0.031
	Enantiomer	1.46	0.240
	Concentration	1.10	0.349
	Interaction	0.0977	0.907

4.2.3| Reproduction parameters

No significant differences were observed for both the number of daphnia with eggs and the number of eggs per daphnia for both enantiomers and racemate (**Figure 21, Table 8**).

Studies have shown that exposure to some drugs such as BE, COC and METH alter the reproductive success of *D. magna* (De Felice et al. 2019, 2020; Parolini et al. 2018). However, no changes in first reproductive events were found to both MDMA racemate and enantiomers on the reproduction of *D. magna*.

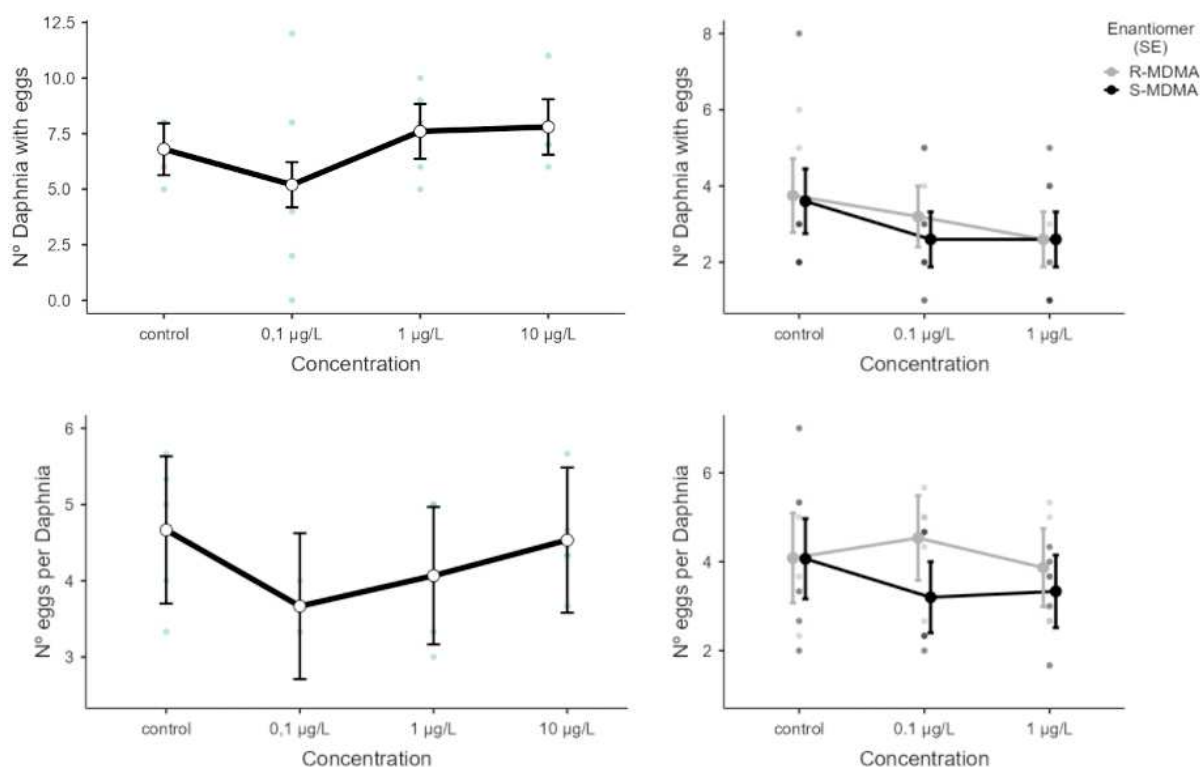


Figure 21 | Effects of MDMA racemate (in the left panel) and enantiomers (in the right panel) on *D. magna* reproduction.

Table 8 | Statistical analysis of effects of MDMA racemate and enantiomers on *D. magna* reproduction.

Variable	Source of variable	χ^2	<i>p</i>
N° daphnia with eggs	<i>rac</i>	3.20	0.362
	Enantiomer	0.149	0.700
	Concentration	1.85	0.396
	Interaction	0.171	0.918
N° eggs per daphnia	<i>rac</i>	0.666	0.881
	Enantiomer	0.764	0.382
	Concentration	0.289	0.866
	Interaction	0.556	0.757

4.2.4 | Biochemical parameters

Studies have shown that exposure to drugs induces oxidative stress and can affect the activity of several enzymes in non-target organisms. Exposure of *D. magna* to BE at concentrations like those found in aquatic ecosystems induces oxidative stress and leads to inhibition of AChE activity (Parolini et al. 2018); similarly, exposure to citalopram and mirtazapine increases levels of ROS and oxidative stress (Duan et al. 2022). In contrast, in our study, no significant changes were found in enzyme levels and ROS. There was

only a significant decrease in AChE and CAT activity in daphnias exposed to the highest concentration of MDMA racemate (**Figure 22, Table 9**). According to Parolini et al. (2018), the activity of AChE enzyme is strictly related to behavioural changes in aquatic organisms, which may explain some of the changes in swimming behaviour found. However, other mechanisms than AChE activity may be involved in changes observed in swimming behaviour.

A reduction in AChE activity in aquatic organisms exposed to environmental pollutants has been attributed to oxidative stress. Although a reduction in AChE enzymatic activity was observed at the highest concentrations (10 µg/L) of the racemate, no increase in ROS levels and indeed a significant decrease in CAT activity was observed at 10 µg/L.

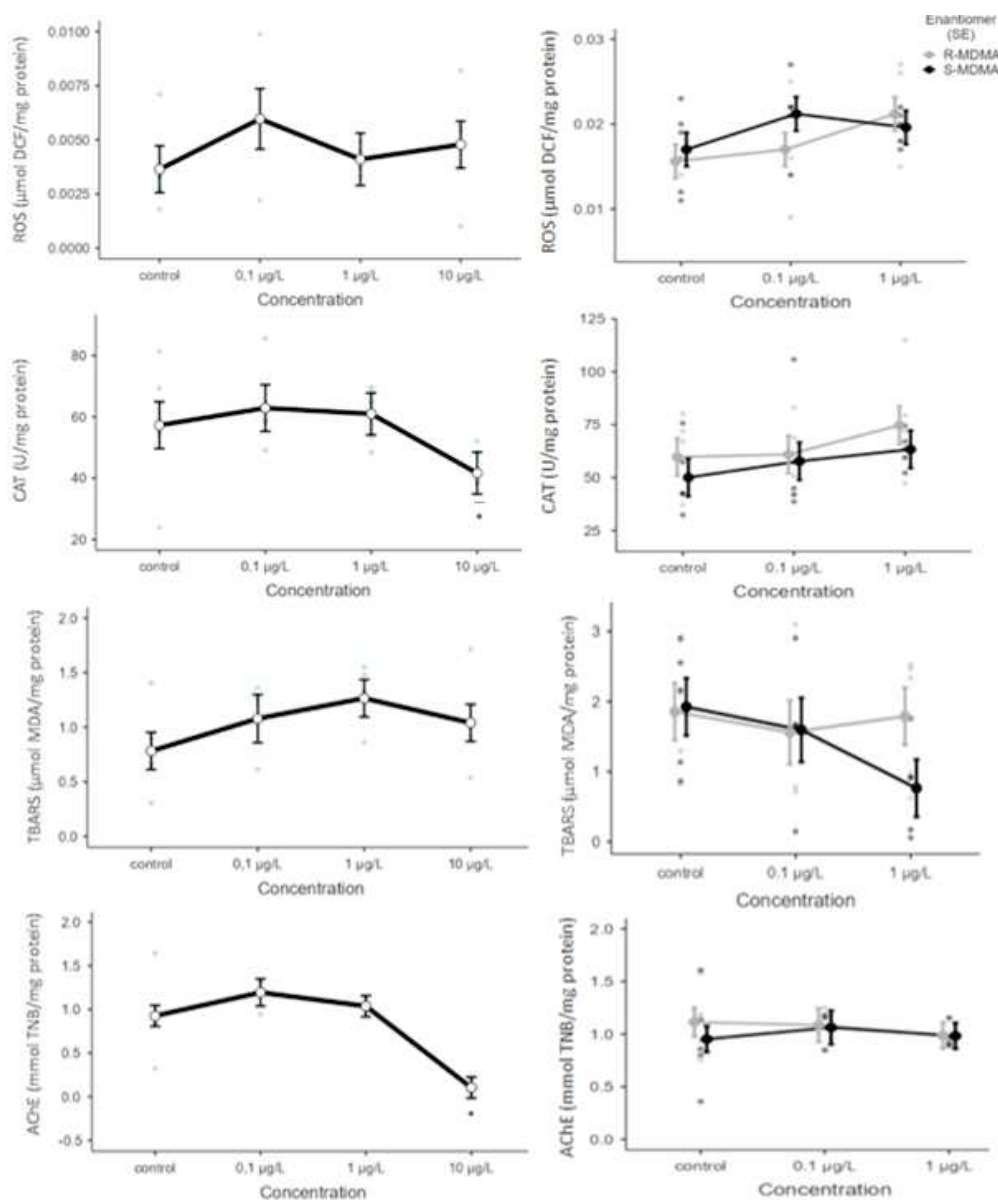


Figure 22 Effects of MDMA racemate (in the left panel) and enantiomers (in the right panel), on biochemical parameters. Note: Asterisks (*) represent significant differences relatively to the control.

Table 9 | Statistical analysis of biochemical effects of MDMA racemate and enantiomers on *D. magna*. Significant effects ($p < 0.05$) in bold.

Variable	Source of variation	<i>F</i>	<i>p</i>
AChE (mmol TNB/mg protein)	<i>rac</i>	48.6	<0.001
	Enantiomer	0.0639	0.804
	Concentration	1.08	0.361
	Interaction	0.0125	0.988
ROS (μmol DCF/mg protein)	<i>rac</i>	0.638	0.604
	Enantiomer	0.669	0.421
	Concentration	2.204	0.132
	Interaction	1.056	0.363
CAT (U/mg protein)	<i>rac</i>	4.39	0.024
	Enantiomer	2.50	0.128
	Concentration	1.41	0.260
	Interaction	0.513	0.605
TBARS (μmol MDA/mg protein)	<i>rac</i>	1.36	0.296
	Enantiomer	0.781	0.386
	Concentration	1.12	0.344
	Interaction	1.12	0.346

5| Conclusions and future perspectives

The possible approval of MDMA to support PTSD treatment might increase its levels in WWTPs and aquatic environments. Thus, enantioselective toxicity tests are necessary for an adequate risk assessment of the occurrence of these substances in the environment.

MDMA is sold in illicit market in the racemate form and enantiomers are not available. Thus, in this study the methodology optimized by Gonçalves et al. (2019) was applied to isolate, the enantiomers for further use in ecotoxicity assays. The semi-preparative method allowed the enantiomers *R*(-)-MDMA and *S*(+)-MDMA in 40.6 % and 2%, respectively. The low recoveries obtained for the *S*(+)-enantiomer, can be explained by the difficulty to prepare the enantiomers due to the formation of an oil, during crystallization which may lead to losses of the substances during the process. Nevertheless, the methodology allowed us to obtain the isolated enantiomers with high enantiomeric purity (>97%) and to proceed with the enantioselective ecotoxicity assays.

The results obtained in this work permit to understand that exposure to MDMA racemate and enantiomers at reported concentrations, can induce significant behavioural and morphophysiological responses and modulation of the CAT and AChE activity in *Daphnia magna*. Body size showed enantioselective effects over time demonstrating the relevance of these studies for an accurate environmental risk assessment. Our results suggest that the *R*(-)-enantiomer is less toxic than the *S*(+)-enantiomer. The *R*(-)-MDMA is the most persistent in the environment and, in this study, no significative changes were found in organisms associated with this enantiomer.

More studies should be carried out considering other biomarkers to increase the knowledge about the impact of MDMA racemate and enantiomers on daphnia and even other non-target organisms. Also, since chemicals do not occur alone in the environment, but together with many other substances, further studies must consider these complex mixtures and the effects that the combination of these contaminants can have in the aquatic environment since they can cause harmful effects on aquatic organisms.

As this substance is expected to increase in the aquatic environment, with potential consequences for aquatic organisms, it is essential that the water quality and environment directive take this into account and adopt measures to mitigate the impact of these substances on the environment and reduce the impacts on animals and humans.

6| Bibliographic references

- Adhikari, Sangeet, Rahul Kumar, Erin M. Driver, Devin A. Bowes, Keng Tiong Ng, Juan Eduardo Sosa-Hernandez, Mariel Araceli Oyervides-Muñoz, Elda M. Melchor-Martínez, Manuel Martínez-Ruiz, Karina G. Coronado-Apodaca, Ted Smith, Aruni Bhatnagar, Brian J. Piper, Kenneth L. McCall, Roberto Parra-Saldivar, Leon P. Barron, and Rolf U. Halden. 2022. “Occurrence of Z-Drugs, Benzodiazepines, and Ketamine in Wastewater in the United States and Mexico during the Covid-19 Pandemic.” *Science of The Total Environment* 159351.
- Alfonso-Prieto, Mercedes, Xevi Biarnés, Pietro Vidossich, and Carme Rovira. 2009. “The Molecular Mechanism of the Catalase Reaction.” *Journal of the American Chemical Society* 131(33):11751–61.
- Antunes, Sara and Bruno Castro. 2017. “Pulgas-de-Água (Daphnia Spp.).” *Revista de Ciência Elementar* 5(4):1–3.
- Bade, Richard, Benjamin J. Tschärke, Jason M. White, Sharon Grant, Jochen F. Mueller, Jake O’Brien, Kevin V. Thomas, and Cobus Gerber. 2019. “LC-HRMS Suspect Screening to Show Spatial Patterns of New Psychoactive Substances Use in Australia.” *Science of The Total Environment* 650:2181–87.
- Baker, David R. and Barbara Kasprzyk-Hordern. 2011. “Multi-Residue Analysis of Drugs of Abuse in Wastewater and Surface Water by Solid-Phase Extraction and Liquid Chromatography–Positive Electrospray Ionisation Tandem Mass Spectrometry.” *Journal of Chromatography A* 1218(12):1620–31.
- Baker, David R. and Barbara Kasprzyk-Hordern. 2013. “Spatial and Temporal Occurrence of Pharmaceuticals and Illicit Drugs in the Aqueous Environment and during Wastewater Treatment: New Developments.” *Science of the Total Environment* 454–455:442–56.
- Barreiro, Juliana Cristina, Maria Elizabeth Tiritan, and Quezia Bezerra Cass. 2021. “Challenges and Innovations in Chiral Drugs in an Environmental and Bioanalysis Perspective.” *TrAC Trends in Analytical Chemistry* 142:116326.
- Bartelt-Hunt, Shannon L., Daniel D. Snow, Teyona Damon, Johnette Shockley, and Kyle Hoagland. 2009. “The Occurrence of Illicit and Therapeutic Pharmaceuticals in Wastewater Effluent and Surface Waters in Nebraska.” *Environmental Pollution* 157(3):786–91.
- Bijlsma, Lubertus, Erik Emke, Félix Hernández, and Pim De Voogt. 2012. “Investigation

- of Drugs of Abuse and Relevant Metabolites in Dutch Sewage Water by Liquid Chromatography Coupled to High Resolution Mass Spectrometry.” *Chemosphere* 89(11):1399–1406.
- Bownik, Adam. 2017. “Daphnia Swimming Behaviour as a Biomarker in Toxicity Assessment: A Review.” *Science of The Total Environment* 601–602:194–205.
- Bownik, Adam. 2020. “Physiological Endpoints in Daphnid Acute Toxicity Tests.” *Science of The Total Environment* 700:134400.
- Campos, Bruno, Danielle Fletcher, Benjamín Piña, Romà Tauler, and Carlos Barata. 2018. “Differential Gene Transcription across the Life Cycle in *Daphnia magna* Using a New All Genome Custom-Made Microarray.” *BMC Genomics* 19(1):1–13.
- Cass, Q. and F. Batigaglia. 2003. “Enantiomeric Resolution of a Series of Chiral Sulfoxides by High-Performance Liquid Chromatography on Polysaccharide-Based Columns with Multimodal Elution.” *Journal of Chromatography A* 987(1–2):445–52.
- Chen, Like, Changsheng Guo, Zhenyu Sun, and Jian Xu. 2021. “Occurrence, Bioaccumulation and Toxicological Effect of Drugs of Abuse in Aquatic Ecosystem: A Review.” *Environmental Research* 200:111362.
- Cruz, Santa, Rick Doblin, Santa Cruz, Amy Emerson, Multi-site Study, Michael C. Mithoefer, and Alia Lilienstein. 2020. *Protocol MAPPI A Randomized , Double-Blind , Placebo-Controlled , Multi-Site Phase 3 Study of the Efficacy and Safety of Manualized MDMA-Assisted Psychotherapy for the Treatment of Severe Posttraumatic Stress Disorder Public MAPPI Protocol Synopsis*.
- Ding, Jiannan, Hua Zou, Qingqing Liu, Shanshan Zhang, and Roger Mamitiana Razanajatovo. 2017. “Bioconcentration of the Antidepressant Fluoxetine and Its Effects on the Physiological and Biochemical Status in *Daphnia Magna*.” *Ecotoxicology and Environmental Safety* 142:102–9.
- Dinis-oliveira, Ricardo Jorge. 2014. “Usos Lícito e Ilícito Dos Fármacos.” 27(6):755–66.
- Duan, Shengzi, Yourong Fu, Shanshan Dong, Yunfeng Ma, Hangyu Meng, Ruixin Guo, Jianqiu Chen, Yanhua Liu, and Yang Li. 2022. “Psychoactive Drugs Citalopram and Mirtazapine Caused Oxidative Stress and Damage of Feeding Behavior in *Daphnia Magna*.” *Ecotoxicology and Environmental Safety* 230:113147.
- European Monitoring Centre of Drug and Drug Addiction. 2020. *European Report of Drugs 2020: Key -issues*. ISBN 978-92-9497-544-7.
- European Monitoring Centre of Drug and Drug Addiction. 2022. *European Report of*

Drugs - Trends and Developments. ISBN 978-92-9497-742-7

- Emke, Erik, Sian Evans, Barbara Kasprzyk-Hordern, and Pim de Voogt. 2014. "Enantiomer Profiling of High Loads of Amphetamine and MDMA in Communal Sewage: A Dutch Perspective." *Science of the Total Environment* 487(1):666–72.
- Evans, S., J. Bagnall, and B. Kasprzyk-Hordern. 2017. "Enantiomeric Profiling of a Chemically Diverse Mixture of Chiral Pharmaceuticals in Urban Water." *Environmental Pollution* 230:368–77.
- Evans, Sian E., John Bagnall, and Barbara Kasprzyk-Hordern. 2016. "Enantioselective Degradation of Amphetamine-like Environmental Micropollutants (Amphetamine, Methamphetamine, MDMA and MDA) in Urban Water." *Environmental Pollution* 215:154–63.
- Evans, Sian E., Paul Davies, Anneke Lubben, and Barbara Kasprzyk-Hordern. 2015. "Determination of Chiral Pharmaceuticals and Illicit Drugs in Wastewater and Sludge Using Microwave Assisted Extraction, Solid-Phase Extraction and Chiral Liquid Chromatography Coupled with Tandem Mass Spectrometry." *Analytica Chimica Acta* 882:112–26.
- Feduccia, Allison A., Julie Holland, and Michael C. Mithoefer. 2018. "Progress and Promise for the MDMA Drug Development Program." *Psychopharmacology* 235:561–571.
- Feduccia, Allison A. and Michael C. Mithoefer. 2018. "MDMA-Assisted Psychotherapy for PTSD: Are Memory Reconsolidation and Fear Extinction Underlying Mechanisms?" *Progress in Neuro-Psychopharmacology and Biological Psychiatry* 84 (March):221–28.
- De Felice, Beatrice, Simona Mondellini, Noelia Salgueiro-González, Sara Castiglioni, and Marco Parolini. 2020. "Methamphetamine Exposure Modulated Oxidative Status and Altered the Reproductive Output in *Daphnia magna*." *Science of the Total Environment* 721:137728.
- De Felice, Beatrice, Noelia Salgueiro-González, Sara Castiglioni, Nicola Saino, and Marco Parolini. 2019. "Biochemical and Behavioral Effects Induced by Cocaine Exposure to *Daphnia magna*." *Science of the Total Environment* 689:141–48.
- Fontanals, N., R. M. Marcé, and F. Borrull. 2017. "Solid-Phase Extraction Followed by Liquid Chromatography-High Resolution Mass Spectrometry to Determine Synthetic Cathinones in Different Types of Environmental Water Samples." *Journal of Chromatography A* 1524:66–73.

- Fontes, Mayana Karoline, Luciane Alves Maranhão, and Camilo Dias Seabra Pereira. 2020. "Review on the Occurrence and Biological Effects of Illicit Drugs in Aquatic Ecosystems." *Environmental Science and Pollution Research* 27(25):30998–34.
- Fraz, Shamaila, Abigail H. Lee, Simon Pollard, Krishna Srinivasan, Abhilasha Vermani, Ephraim David, and Joanna Y. Wilson. 2019. "Paternal Exposure to Carbamazepine Impacts Zebrafish Offspring Reproduction Over Multiple Generations." *Environmental Science & Technology* 53(21):12734–43.
- Ghani, Md Ahsan, Celia Barril, Danny R. Bedgood, and Paul D. Prenzler. 2017. "Measurement of Antioxidant Activity with the Thiobarbituric Acid Reactive Substances Assay." *Food Chemistry* 230:195–207.
- Gonçalves, Ricardo, Cláudia Ribeiro, Sara Cravo, Sara C. Cunha, José Augusto Pereira, J. O. Fernandes, Carlos Afonso, and Maria Elizabeth Tiritan. 2019. "Multi-Residue Method for Enantioseparation of Psychoactive Substances and Beta Blockers by Gas Chromatography–Mass Spectrometry." *Journal of Chromatography B: Analytical Technologies in the Biomedical and Life Sciences* 1125:121731.
- Gustinasari, Kiki, Łukasz Ślugocki, Robert Czerniawski, Ellina S. Pandebesie, and Joni Hermana. 2021. "Acute Toxicity and Morphology Alterations of Glyphosate-Based Herbicides to *Daphnia magna* and *Cyclops vicinus*." *Toxicological Research* 37(2):197–207.
- Hadwan, Mahmoud Hussein. 2018. "Simple Spectrophotometric Assay for Measuring Catalase Activity in Biological Tissues." *BMC Biochemistry* 19(1):7.
- Hernández, F., M. Ibáñez, R. Bade, L. Bijlsma, and J. V. Sancho. 2014. "Investigation of Pharmaceuticals and Illicit Drugs in Waters by Liquid Chromatography-High-Resolution Mass Spectrometry." *TrAC - Trends in Analytical Chemistry* 63:140–57.
- Hubert, Cécile, Martin Roosen, Yves Levi, and Sara Karolak. 2017. "Validation of an Ultra-High-Performance Liquid Chromatography-Tandem Mass Spectrometry Method to Quantify Illicit Drug and Pharmaceutical Residues in Wastewater Using Accuracy Profile Approach." *Journal of Chromatography A* 1500:136–44.
- Huerta-Fontela, Maria, Maria Teresa Galceran, Jordi Martin-Alonso, and Francesc Ventura. 2008. "Occurrence of Psychoactive Stimulatory Drugs in Wastewaters in North-Eastern Spain." *Science of the Total Environment* 397(1–3):31–40.
- Huerta-Fontela, Maria, Maria Teresa Galceran, and Francesc Ventura. 2008. "Stimulatory Drugs of Abuse in Surface Waters and Their Removal in a Conventional Drinking Water Treatment Plant." *Environmental Science and Technology* 42(18):6809–16.

- Jin, Hangbiao, Dan Yang, Pengfei Wu, and Meirong Zhao. 2022. “Environmental Occurrence and Ecological Risks of Psychoactive Substances.” *Environment International* 158(October 2021):106970.
- Karolak, Sara, Thomas Nefau, Emilie Bailly, Audrey Solgadi, and Yves Levi. 2010. “Estimation of Illicit Drugs Consumption by Wastewater Analysis in Paris Area (France).” *Forensic Science International* 200(1–3):153–60.
- Kasprzyk-Hordern, Barbara, Vishnu V. R. Kondakal, and David R. Baker. 2010. “Enantiomeric Analysis of Drugs of Abuse in Wastewater by Chiral Liquid Chromatography Coupled with Tandem Mass Spectrometry.” *Journal of Chromatography A* 1217(27):4575–86.
- Kaushik, Gaurav and Michael A. Thomas. 2019. “The Potential Association of Psychoactive Pharmaceuticals in the Environment with Human Neurological Disorders.” *Sustainable Chemistry and Pharmacy* Volume 13(100148).
- Li, Kaiyang, Peng Du, Zeqiong Xu, Tingting Gao, and Xiqing Li. 2016. “Occurrence of Illicit Drugs in Surface Waters in China.” *Environmental Pollution* 213:395–402.
- Li, Meifeng, Tingting Yu, Jingli Lai, Xue Han, Jihuan Hu, Zeyuan Deng, Dongming Li, Zuocheng Ye, Shanghong Wang, Chengyu Hu, and Xiaowen Xu. 2021. “Ethoprophos Induces Cardiac Toxicity in Zebrafish Embryos.” *Ecotoxicology and Environmental Safety* 228:113029.
- Li, Shih-Wei, Yu-Hsiang Wang, and Angela Yu-Chen Lin. 2017. “Ecotoxicological Effect of Ketamine: Evidence of Acute, Chronic and Photolysis Toxicity to *Daphnia magna*.” *Ecotoxicology and Environmental Safety* 143:173–79.
- Li, Y. Robert and Michael Trush. 2016. “Defining ROS in Biology and Medicine.” *Reactive Oxygen Species* 1(1).
- Lin, Angela Yu-Chen, Wan-Ning Lee, and Xiao-Huan Wang. 2014. “Ketamine and the Metabolite Norketamine: Persistence and Phototransformation Toxicity in Hospital Wastewater and Surface Water.” *Water Research* 53:351–60.
- Lionetto, Maria Giulia, Roberto Caricato, Antonio Calisi, Maria Elena Giordano, and Trifone Schettino. 2013. “Acetylcholinesterase as a Biomarker in Environmental and Occupational Medicine: New Insights and Future Perspectives.” *BioMed Research International* 2013:1–8.
- Mackul’ak, Tomáš, Lucia Birošová, Igor Bodík, Roman Grabic, Alžbeta Takáčová, Miroslava Smolinská, Anna Hanusová, Ján Híveš, and Miroslav Gál. 2016. “Zerovalent Iron and Iron(VI): Effective Means for the Removal of Psychoactive

- Pharmaceuticals and Illicit Drugs from Wastewaters.” *Science of The Total Environment* 539:420–26.
- MAPS. n.d. “Inverse: MDMA Steps Closer to FDA Approval as a Drug, but Now It Needs to Leap.” Retrieved (<https://maps.org/articles/6094-inverse-mdma-steps-closer-to-fda-approval-as-a-drug,-but-now-it-needs-to-leap>).
- Mitchell, Jennifer M., Michael Bogenschutz, Alia Lilienstein, Charlotte Harrison, Sarah Kleiman, Kelly Parker-Guilbert, Marcela Ot’alora G., Wael Garas, Casey Paleos, Ingmar Gorman, Christopher Nicholas, Michael Mithoefer, Shannon Carlin, Bruce Poulter, Ann Mithoefer, Sylvestre Quevedo, Gregory Wells, Sukhpreet S. Klaire, Bessel van der Kolk, Keren Tzarfaty, Revital Amiaz, Ray Worthy, Scott Shannon, Joshua D. Woolley, Cole Marta, Yevgeniy Gelfand, Emma Hapke, Simon Amar, Yair Wallach, Randall Brown, Scott Hamilton, Julie B. Wang, Allison Coker, Rebecca Matthews, Alberdina de Boer, Berra Yazar-Klosinski, Amy Emerson, and Rick Doblin. 2021. “MDMA-Assisted Therapy for Severe PTSD: A Randomized, Double-Blind, Placebo-Controlled Phase 3 Study.” *Nature Medicine* 27(6):1025–33.
- Mithoefer, Michael C. 2017. “A Manual for MDMA-Assisted Psychotherapy in the Treatment of Posttraumatic Stress Disorder.” 75.
- Mithoefer, Michael C., Ann T. Mithoefer, Allison A. Feduccia, Lisa Jerome, Mark Wagner, Joy Wymer, Julie Holland, Scott Hamilton, Berra Yazar-Klosinski, Amy Emerson, and Rick Doblin. 2018. “3,4-Methylenedioxymethamphetamine (MDMA)-Assisted Psychotherapy for Post-Traumatic Stress Disorder in Military Veterans, Firefighters, and Police Officers: A Randomised, Double-Blind, Dose-Response, Phase 2 Clinical Trial.” *The Lancet Psychiatry* 5(6):486–97.
- Mithoefer, Michael C., Mark T. Wagner, Ann T. Mithoefer, Lisa Jerome, Scott F. Martin, Berra Yazar-Klosinski, Yvonne Michel, Timothy D. Brewerton, and Rick Doblin. 2013. “Durability of Improvement in Post-Traumatic Stress Disorder Symptoms and Absence of Harmful Effects or Drug Dependency after 3,4-Methylenedioxymethamphetamine-Assisted Psychotherapy: A Prospective Long-Term Follow-up Study.” *Journal of Psychopharmacology* 27(1):28–39.
- Nehate, Sagar P., Himanshu M. Godbole, Girij P. Singh, Jessy E. Mathew, and Gautham G. Shenoy. 2018. “Synthesis of Novel Class of 2-Oxazolidinone Based Chiral Ionic Liquids.” *Synthetic Communications* 48(18):2435–40.
- Nilsen, Elena, Kelly L. Smalling, Lutz Ahrens, Meritxell Gros, Karina S. B. Miglioranza, Yolanda Picó, and Heiko L. Schoenfuss. 2019. “Critical Review: Grand Challenges

- in Assessing the Adverse Effects of Contaminants of Emerging Concern on Aquatic Food Webs.” *Environmental Toxicology and Chemistry* 38(1):46–60.
- OECD, Organization of Economic Co-operation and Development D. 2004. “Test No. 211: *Daphnia magna* Reproduction Test.” *Test No. 211: Daphnia magna Reproduction Test* (Abril).
- Observatório Europeu da Droga e Toxicodependência. 2021. *Relatório Europeu Sobre Drogas 2021 : Tendências e Evoluções*. Serviço das Publicações da União Europeia, Luxemburgo. ISBN 978-92-9497-588-1
- Observatório Europeu da Droga e da Toxicodependência. 2014. “Relatório Europeu Sobre Drogas - Tendências e Evoluções.” Serviço das Publicações da União Europeia, Luxemburgo. (351):21–23, ISBN: 978-92-9168-707-7
- Parolini, Marco, Beatrice De Felice, Claudia Ferrario, Noelia Salgueiro-González, Sara Castiglioni, Antonio Finizio, and Paolo Tremolada. 2018. “Benzoylcegonine Exposure Induced Oxidative Stress and Altered Swimming Behavior and Reproduction in *Daphnia magna*.” *Environmental Pollution* 232:236–44.
- Parolini, Marco, Stefano Magni, Sara Castiglioni, and Andrea Binelli. 2016. “Amphetamine Exposure Imbalanced Antioxidant Activity in the Bivalve *Dreissena polymorpha* Causing Oxidative and Genetic Damage.” *Chemosphere* 144:207–13.
- Pérez-Pereira, Ariana, Cláudia Ribeiro, Filomena Teles, Ricardo Gonçalves, Virgínia M.F. Gonçalves, José Augusto Pereira, João Soares Carrola, Carlos Pires, and Maria Elizabeth Tiritan. 2022. “Ketamine and Norketamine: Enantioresolution and Enantioselective Aquatic Ecotoxicity Studies.” *Environmental Toxicology and Chemistry* 41(3):569–79.
- Pérez, Héctor López, D. Farfan, M. Garzón, Ministerio de Educación Nacional, Kimiz Dalker, Manuel Alfonso Garzón Castrillón, Departamento Administrativo de la Función Pública, Comisión Intersectorial de Estadísticas de Finanzas Públicas [CIEFP], Departamento Administrativo de la Función Pública, Peter F. Drucker, Jim Botkin, Ministerio de Educación Nacional, Consejo Nacional Legislativo, Ministerio de Educación Nacional, Duván Emilio Ramírez Ospina, Leif. Edvinsson, Michael S. Malone, Jim Botkin, Jorge Raul Muñate Diaz, Israel Núñez, Oscar Hauptman, Jeremy Neuringer, Ikujiro Nonaka, Hirotaka. Takeuchi, Katia Franch León, Vivian Antúnez Saiz, Katy Herrera Lemus, Israel A. Núñez Paula, Yiny Núñez Govín, César Lambert, Felipe Salazar Pinzon, Nelson Antonio Quintanilla Juárez, Ernesto Galvis-Lista, Escuela Interamericana, Sonia Lucia, Rosero Jiménez,

- Herlayne Segura Jiménez, Gestión D. E. L. Conocimiento, César Lambert, Mercedes Segarra, Juan Bou., Pedagógico De Barquisimeto, Upel Ipb, Carlos Eduardo, Marulanda Echeverry, Ingeniero Industrial, C. A. D. Cam, El Modelo, Canadian Imperial, El Modelo Intellect, A. J. Sánchez Medina, A. Melián González, E. Hormiga Pérez, Carlos Eduardo, Marulanda Echeverry, Ingeniero Industrial, C. A. D. Cam, El Modelo, Canadian Imperial, El Modelo Intellect, Guillermo Correa Uribe, Sonia Lucia Rosero Jimenez, Herlayne Segura Jimenez, Daniel Pérez, Matthias Dressler, Manuel Alfonso Garzón Castrillón, Sistema De Gestión, Nofal Nagles G., Israel A. Núñez Paula, Kimiz Dalkir, D. Farfan, M. Garzón, Carolina Mejía, Ramon Fabregat, Daniel Salas, Katia Franch León, Vivian Antúnez Saiz, Katy Herrera Lemus, Israel Núñez, Alvin Toffler, Heidi Toffler, Peter F. Drucker, Departamento Administrativo de la Función Pública, Gestión Del, Conocimiento E. Innovación, Objetivo Del, S. I. G. Que, Departamento Administrativo de la Función Pública, Productividad Del, Trabajador Del, Ministerio de Educación Nacional, Kimiz Dalker, JAVIER DARÍO ACOSTA MARÍN, Mónica Cristina, Hernández Muñoz, Daniel Pérez, and Matthias Dressler. 2005. "Manual Operativo." *Acimed* 12(3):73.
- Petrie, Bruce, Jana Mrazova, Barbara Kasprzyk-Hordern, and Kyari Yates. 2018. "Multi-Residue Analysis of Chiral and Achiral Trace Organic Contaminants in Soil by Accelerated Solvent Extraction and Enantioselective Liquid Chromatography Tandem–Mass Spectrometry." *Journal of Chromatography A* 1572:62–71.
- Pizarro, Nieves, Magí Farré, Mitona Pujadas, Ana Ma Peiró, Pere N. Roset, Jesús Joglar, and Rafael de la Torre. 2004. "Stereochemical Analysis of 3,4-Methylenedioxyamphetamine and Its Main Metabolites in Human Samples Including the Catechol-Type Metabolite (3,4-Dihydroxyamphetamine)." *Drug Metabolism and Disposition: The Biological Fate of Chemicals* 32(9):1001–7.
- Pizarro, Nieves, Amadeu Llebaria, Silvia Cano, Jesús Joglar, Magí Farré, Jordi Segura, and Rafael de la Torre. 2003. "Stereochemical Analysis of 3,4-Methylenedioxyamphetamine and Its Main Metabolites by Gas Chromatography/Mass Spectrometry." *Rapid Communications in Mass Spectrometry* 17(4):330–36.
- Pourahmad, Jalal, Peter J. O'Brien, Farzaneh Jokar, and Bahram Daraei. 2003. "Carcinogenic Metal Induced Sites of Reactive Oxygen Species Formation in Hepatocytes." *Toxicology in Vitro* 17(5–6):803–10.

- Ribeiro, Ana Rita L., Alexandra S. Maia, Cláudia Ribeiro, and Maria Elizabeth Tiritan. 2020. "Analysis of Chiral Drugs in Environmental Matrices: Current Knowledge and Trends in Environmental, Biodegradation and Forensic Fields." *TrAC Trends in Analytical Chemistry* 124:115783.
- Ribeiro, Cláudia, Ana Ribeiro, Alexandra Maia, and Maria Tiritan. 2017. "Occurrence of Chiral Bioactive Compounds in the Aquatic Environment: A Review." *Symmetry* 9(10):215.
- Ribeiro, Cláudia, Ana Rita Ribeiro, and Maria Elizabeth Tiritan. 2016. "Priority Substances and Emerging Organic Pollutants in Portuguese Aquatic Environment: A Review." Pp. 1–44 in.
- Ribeiro, Cláudia, Cristiana Santos, Valter Gonçalves, Ana Ramos, Carlos Afonso, and Maria Elizabeth Tiritan. 2018. "Chiral Drug Analysis in Forensic Chemistry: An Overview." *Molecules* 23(2).
- Ribeiro, Ondina, Luís Félix, Cláudia Ribeiro, Bruno Castro, Maria Elizabeth Tiritan, Sandra Mariza Monteiro, and João Soares Carrola. 2022. "Enantioselective Ecotoxicity of Venlafaxine in Aquatic Organisms: Daphnia and Zebrafish." *Environmental Toxicology and Chemistry* 41(8):1851–64.
- Ribeiro, Ondina Martins Ribeiro, Mónica Quelhas Pinto Pinto, Cláudia Ribeiro Ribeiro, Maria Elizabeth Tiritan Tiritan, and João Soares Carrola Carrola. 2021. "A Dáfnia Como Sensor Da Ecotoxicidade." *Revista de Ciência Elementar* 9(2):1–6.
- Rodríguez-Fuentes, Gabriela, Fernando J. Rubio-Escalante, Elsa Noreña-Barroso, Karla S. Escalante-Herrera, and Daniel Schlenk. 2015. "Impacts of Oxidative Stress on Acetylcholinesterase Transcription, and Activity in Embryos of Zebrafish (Danio Rerio) Following Chlorpyrifos Exposure." *Comparative Biochemistry and Physiology Part C: Toxicology & Pharmacology* 172–173:19–25.
- Salgueiro-González, Noelia, Sara Castiglioni, Emma Gracia-Lor, Lubertus Bijlsma, Alberto Celma, Renzo Bagnati, Félix Hernández, and Ettore Zuccato. 2019. "Flexible High Resolution-Mass Spectrometry Approach for Screening New Psychoactive Substances in Urban Wastewater." *Science of The Total Environment* 689:679–90.
- Sessa, Ben. 2017. "MDMA and PTSD Treatment: 'PTSD: From Novel Pathophysiology to Innovative Therapeutics.'" *Neuroscience Letters* 649:176–80.
- Silman, Israel and Joel L. Sussman. 2008. "Acetylcholinesterase: How Is Structure Related to Function?" *Chemico-Biological Interactions* 175(1–3):3–10.

- Skees, Allie J., Katelyn S. Foppe, Bommanna Loganathan, and Bikram Subedi. 2018. "Contamination Profiles, Mass Loadings, and Sewage Epidemiology of Neuropsychiatric and Illicit Drugs in Wastewater and River Waters from a Community in the Midwestern United States." *Science of The Total Environment* 631–632:1457–64.
- Stewart, Adam, Russell Riehl, Keith Wong, Jeremy Green, Jessica Cosgrove, Karoly Vollmer, Evan Kyzar, Peter Hart, Alexander Allain, Jonathan Cachat, Siddharth Gaikwad, Molly Hook, Kate Rhymes, Alan Newman, Eli Utterback, Katie Chang, and Allan V Kalueff. 2012. "Behavioral Effects of MDMA ('Ecstasy') on Adult Zebrafish." *Behavioral Pharmacology* 22(3):275–80.
- Szabelak, Aleksandra and Adam Bownik. 2021. "Behavioral and Physiological Responses of *Daphnia Magna* to Salicylic Acid." *Chemosphere* 270:128660.
- Tachibana, Kozo and Atsushi Ohnishi. 2001. "Reversed-Phase Liquid Chromatographic Separation of Enantiomers on Polysaccharide Type Chiral Stationary Phases." *Journal of Chromatography A* 906(1–2):127–54.
- Teixeira, Joana, Maria Elizabeth Tiritan, Madalena M. M. Pinto, and Carla Fernandes. 2019. "Chiral Stationary Phases for Liquid Chromatography: Recent Developments." *Molecules* 24(5):865.
- Tiritan, Maria E., Carla Fernandes, Alexandra S. Maia, Madalena Pinto, and Quezia B. Cass. 2018. "Enantiomeric Ratios: Why so Many Notations?" *Journal of Chromatography A* 1569:1–7.
- Tiritan, Maria Elizabeth, Ana Rita Ribeiro, Carla Fernandes, and Madalena M. M. Pinto. 2016. "Chiral Pharmaceuticals." Pp. 1–28 in *Kirk-Othmer Encyclopedia of Chemical Technology*. Vol. 20. Hoboken, NJ, USA: John Wiley & Sons, Inc.
- Tkaczyk, Angelika, Adam Bownik, Jarosław Dudka, Krzysztof Kowal, and Brygida Ślaska. 2021. "*Daphnia Magna* Model in the Toxicity Assessment of Pharmaceuticals: A Review." *Science of The Total Environment* 763:143038.
- Tsikis, Dimitrios. 2017. "Assessment of Lipid Peroxidation by Measuring Malondialdehyde (MDA) and Relatives in Biological Samples: Analytical and Biological Challenges." *Analytical Biochemistry* 524:13–30.
- Valko, Marian, Klaudia Jomova, Christopher J. Rhodes, Kamil Kuča, and Kamil Musílek. 2016. "Redox- and Non-Redox-Metal-Induced Formation of Free Radicals and Their Role in Human Disease." *Archives of Toxicology* 90(1):1–37.

- Vazquez-Roig, Pablo, Barbara Kasprzyk-Hordern, Cristina Blasco, and Yolanda Picó. 2014. “Stereoisomeric Profiling of Drugs of Abuse and Pharmaceuticals in Wastewaters of Valencia (Spain).” *Science of the Total Environment* 494–495:49–57.
- Yang, Bowen, Yu Chen, and Jianlin Shi. 2019. “Reactive Oxygen Species (ROS)-Based Nanomedicine.” *Chemical Reviews* 119(8):4881–4985.
- Yang, Shenshu and Gaojian Lian. 2020. “ROS and Diseases: Role in Metabolism and Energy Supply.” *Molecular and Cellular Biochemistry* 467(1–2):1–12.
- Zhao, Pengfei, Zhaokun Wang, Kunjie Li, Xingjie Guo, and Longshan Zhao. 2018. “Multi-Residue Enantiomeric Analysis of 18 Chiral Pesticides in Water, Soil and River Sediment Using Magnetic Solid-Phase Extraction Based on Amino Modified Multiwalled Carbon Nanotubes and Chiral Liquid Chromatography Coupled with Tandem Mass Spectrometry.” *Journal of Chromatography A* 1568:8–21.

Note: The bibliography was formatted with Mendeley using the style of *American Sociological Journal*.

7| Attachments

Annex I – Abstract and Poster communication presented in APCF-TOXRUN International Congress 2022.

POSTER

MDMA EFFECTS ON *DAPHNIA MAGNA* MORPHOPHYSIOLOGY – PRELIMINARY DATA

Ana Costa^{1*}, Ariana Pérez-Pereira^{1,2}, Ana Carvalho¹, Bruno Castro^{3,4}, João Carrola², Maria Tiritan^{1,5,6}, Cláudia Ribeiro^{1,5}

¹TOXRUN – Toxicology Research Unit, University Institute of Health Sciences, IUCS-CESPU, CRL, 4585-116 Gandra, Portugal.

²Department of Biology and Environment, University of Trás-os-Montes and Alto Douro, CITAB, Vila Real, Portugal.

³CBMA (Centre of Molecular and Environmental Biology), Department of Biology, University of Minho, Braga, Portugal.

⁴Institute of Science and Innovation for Bio-Sustainability (IB-S), University of Minho, Braga, Portugal.

⁵Interdisciplinary Center of Marine and Environmental Research (CIIMAR), University of Porto, Edifício do Terminal de Cruzeiros do Porto de Leixões, Matosinhos, Portugal.

⁶Laboratory of Organic and Pharmaceutical Chemistry, Department of Chemical Sciences, Faculty of Pharmacy, University of Porto, Portugal.

*Email: a29445@alunos.cespu.pt

Introduction: The presence of psychoactive substances (PAS) in aquatic ecosystems has been frequently documented. PAS are excreted in urine and can reach wastewater effluents ending in aquatic ecosystems posing unpredictable adverse effects on non-target organisms, including microcrustaceans, due to their capacity to interfere with the biochemical, cellular, physiological and behavioral mechanisms [1-3]. Recently, clinical research for the possible use of 3,4-methylenedioxymethamphetamine (MDMA) as an adjunct to psychotherapy in patients with post-traumatic stress disorder has increased [4]. Additionally, the possible approval of MDMA-assisted psychotherapy may cause an increase in its occurrence in aquatic ecosystems.

Objectives: The main objective of this work is to evaluate MDMA effects in *Daphnia magna* as an ecologically relevant model focusing on morphophysiological parameters.

Methods: Groups of 15 neonates with less than 24 hours were randomly distributed and exposed to 0, 0.1, 1 and 10 µg/L MDMA for 8 days, with total of 5 replica. On day 3 and 8 of exposure, morphophysiological parameters (body size, heart size and area) were determined using a microscope with digital camera, and images were processed with specific software to perform the detailed measurements.

Results: No morphological changes were observed at the lowest MDMA concentration (0.1 µg/L). However, in the first days of exposure and at the highest concentration, changes in morphophysiological parameters were found. A decreasing tendency in daphnia size, heart area and size was observed in animals exposed to the higher concentrations (1 and 10 µg/L). However, careful considerations should be taken because all endpoints have not yet been analysed.

Conclusion: The conceivable approval of psychotherapy with MDMA, with an expected increase of MDMA in the aquatic ecosystem, may cause deleterious effects on the morphophysiology of *D. magna* but more studies are necessary to confirm these effects at both sub-chronic and chronic exposures for a deeper knowledge of the possible impact of MDMA in this organism.

Keywords:

MDMA; ecotoxicity; *Daphnia magna*; psychoactive drugs

Acknowledgments: This work is supported by national funds through the FCT/MCTES (PIDDAC), under the project PTDC/CTA-AMB/6686/2020. A. Pérez-Pereira acknowledges the PhD grant BD/CBAS/CESPU/04/2022.

References:

1. Lai FY, O'Brien JW, Thai PK, Hall W, Chan G, Bruno R, Ort C, Prichard J, Carter S, Anuj S, Kirkbride KP, Gartner C, Humphries M, Mueller JF. Cocaine, MDMA and methamphetamine residues in wastewater: Consumption trends (2009–2015) in South East Queensland, Australia. *Sci Total Environ* 588: 803–809, 2018.
2. Parolini M, Felice BD, Ferrario C, Salgueiro-González N, Castiglioni S, Finizio A, Tremolada P. Benzoyllecgonine exposure induced oxidative stress and altered swimming behavior and reproduction in *Daphnia magna*. *Environ Poll* 232: 236–244, 2018.
3. Felice BD, Mondellini S, Salgueiro-González N, Castiglioni S, Parolini M. Methamphetamine exposure modulated oxidative status and altered the reproductive output in *Daphnia magna*. *Sci Total Environ* 721: 137728, 2020.
4. Doblin R, Cruz S, Emerson A, Michael C, Lillenstein A. Protocol MAPP1 A Randomized, Double-Blind, Placebo-Controlled, Multi-Site Phase 3 Study of the Efficacy and Safety of Manualized MDMA-Assisted Psychotherapy for the Treatment of Severe Posttraumatic Stress Disorder Public MAPP1 Protocol Synopsis: 86, 2020.

MDMA EFFECTS ON *DAPHNIA MAGNA* MORPHOPHYSIOLOGY - PRELIMINARY DATA

Ana Costa^{1*}, Ariana Pérez-Pereira^{1,2}, Ana Carvalho¹, Bruno Castro^{3,4}, João Carroia², Maria Tirtan^{1,5,6}, Cláudia Ribalro^{1,6}

¹TORLIM – Toxicology Research Unit, University Institute of Health Sciences, IUCS-CESPU, OLS, Gandra, Portugal; ²Department of Biology and Environment, University of Trás-os-Montes and Alto Alentejo, CITAF, Vila Real, Portugal; ³CEMMA (Centre of Molecular and Environmental Biology), Department of Biology, University of Minho, Braga, Portugal; ⁴Institute of Science and Innovation for Bio-Sustainability (IS-BS), University of Minho, Braga, Portugal; ⁵Interdisciplinary Center of Marine and Environmental Research (CIMAR), University of Porto, Matosinhos, Portugal; ⁶Laboratory of Organic and Pharmaceutical Chemistry, Department of Chemical Sciences, Faculty of Pharmacy, University of Porto, Portugal



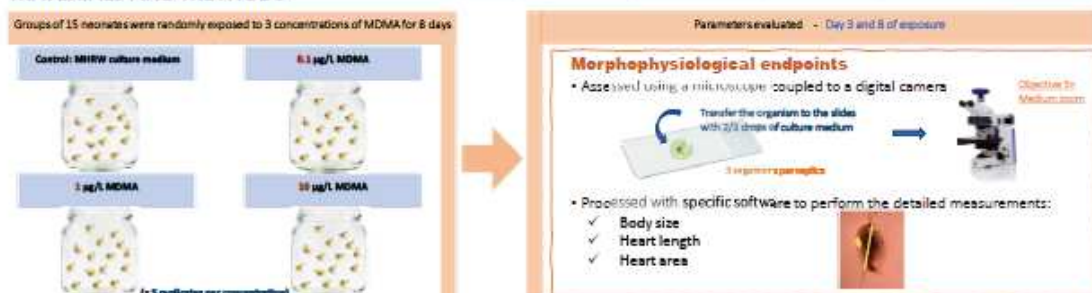
INTRODUCTION

The presence of psychoactive substances (PAS) in aquatic ecosystems has been frequently documented [1]. PAS are excreted in urine and have been detected in effluents ending up in the aquatic ecosystems. Thereby, PAS may pose unpredictable adverse effects on non-target organisms due to their capacity to interfere with the biochemical, cellular, physiological and behavioral mechanisms [1-3]. Recently, clinical research for the possible use of 3,4-methylenedioxymethamphetamine (MDMA) as an adjunct to

psychotherapy in patients with post-traumatic stress disorder has increased [4]. Additionally, the possible approval of MDMA-assisted psychotherapy may increase its occurrence in aquatic ecosystems.

Therefore, this study aimed to evaluate MDMA effects in *Daphnia magna* as an ecologically relevant model focusing on several morphophysiological parameters: body size, heart length and area.

MATERIALS AND METHODS



RESULTS AND DISCUSSION

In the first 3 days of exposure and at the highest concentration, changes in morphophysiological parameters were found. A decreasing tendency in daphnia body size, heart area and size was observed in animals exposed to the higher concentrations (1 and 10 µg/L) (Figure 1, 2 and 3). On day 8, no differences were found on these morphophysiological parameters (Figure 1, 2 and 3). However, careful considerations should be taken as the other endpoints have not yet been analyzed.

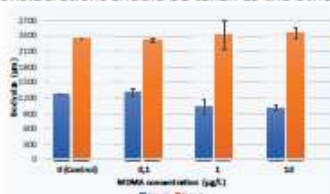


Figure 1: Comparison of body size (µm) at day 3 and 8 of exposure to different concentrations of MDMA.

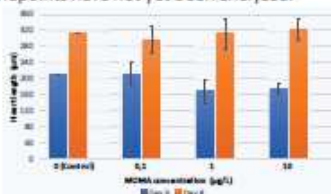


Figure 2: Comparison of heart length (µm) at day 3 and 8 of exposure to different concentrations of MDMA.

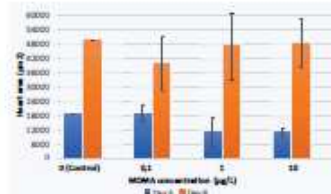


Figure 3: Comparison of heart area (µm²) at day 3 and 8 of exposure to different concentrations of MDMA.

CONCLUSIONS

The conceivable approval of psychotherapy with MDMA, with an expected increase of MDMA in the aquatic ecosystem, may have consequences on the morphophysiology of *D. magna* especially in the first days of contact with the drug. But on day 8, organisms appear to have acquired the ability to adapt to MDMA exposure. Nevertheless, more studies are necessary to confirm these effects at both sub-chronic and chronic exposures and deep knowledge about the possible impact of MDMA in this organism.

REFERENCES

1. Liu PY, O'Brien JW, The PH, Hill W, Chan S, Burns R, Orr C, Pritchard J, Coker B, Any B, Kibrosey NP, Gattner C, Kociprowski M, Mueller JF, Coakley, MDMA and methamphetamine residues in wastewater: Consumption trends (2008-2017) in South West Queensland, Australia. Sci Total Environ. 653-654, 2019.
2. Perillo M, Felice SG, Ferraro C, Seguelo-García R, Castiglioni B, Pirota A, Terranova P. Neuroplasticity exposure induced oxidative stress and altered learning behavior and apoptosis in *Daphnia magna*. Environ. Toxicol. 2020; 35:202-206-214, 2020.
3. Felice SG, Maddaloni B, Seguelo-García R, Castiglioni B, Perillo M. Methamphetamine exposure modulated oxidative stress and altered the reproductive output in *Daphnia magna*. Sci Total Environ. 721-132726, 2020.
4. Doblin R, Chiz S, Gonzalez A, Wehrli C, Liberman A. Protocol MAPPI (Randomized, Double-blind, Placebo-Controlled, Multi-Dose Phase 3 Study of the Efficacy and Safety of Methylphenidate Assisted Psychotherapy for the Treatment of Severe Posttraumatic Stress Disorder. Public Health. Preprint bioRxiv. 2020.

Funding: This work is financially supported by national funds through the FCT/MCTES (PIDDAC), under the project PTDC/C1A-AMB/1995/2020 and partially supported by national funds by FCT - Foundation for Science and Technology through the projects UIDB/04423/2020 and UIDP/04423/2020 (Group of Natural Products and Medicinal Chemistry).

Acknowledgments: To project UIDB/04423/2020 and A. Felice-Pereira acknowledges the PhD grant BQ/CBAS/CESPU/04/2022.



Annex II – Stock solutions for preparation of *R. subcapitata* culture medium.

The **micronutrient stock solution** was prepared by adding the following nutrients to a volumetric flask (250mL) with distilled water: 46.38 mg of H₃BO₃; 103.85 mg of MnCl₂.4H₂O; 0.818 mg of ZnCl₂; 39.94 mg of FeCl₃.6H₂O; 0.357 mg of CoCl₂.6H₂O; 1.815 mg of Na₂MoO₄.2H₂O; and 75.0 mg of Na₂EDTA.2H₂O. When ready, the solution was stored in an amber bottle at 4°C.

Individual macronutrient stock solutions were prepared in 100mL of distilled water. The solutions contained: 2.55 g of NaNO₃; 1.22 g of MgCl₂.6H₂O; 0.441 g of CaCl₂.2H₂O; 1.47 g of MgSO₄.7H₂O; 0.1044 g of K₂HPO₄; and 1.500 g of NaHCO₃. They were stored in amber bottles at 4°C.

For a 1 L glass bottle with distilled water, 1 mL of each macronutrient stock solution was added (except the NaHCO₃ solution, which was only added after autoclaving the culture medium). The medium is autoclaved at 121°C for 15 minutes and then, 1 mL of the micronutrient stock solution and of the macronutrient NaHCO₃ stock solution is added and the pH adjusted (7.5 ± 0.1).

Annex III – Preparation of standards and samples for biochemical assays.

Table 10| Preparation of standards for BSA calibration curve.

BSA standards	Cf BSA (mg/mL)	Vi BSA (µL)	PBS (pH 7.4) (µL)	Bradford Reagent (µL)
Blank	0	0	100	100
1	0.0005	1	99	
2	0.0010	2	98	
3	0.0015	3	97	
4	0.0030	6	94	
5	0.0045	9	91	
6	0.0060	12	88	
7	0.0075	15	85	

Table 11| Preparation of standards for DCF calibration curve.

BSA standards	Cf DCF (μM)	Vi DCF (μL)	PBS (pH 7.4) (μL)
Blank	0	20	100
1	0.078125		
2	0.15625		
3	0.3125		
4	0.625		
5	1.25		
6	2.5		
7	5		
8	10		
9	20		

Table 12| Preparation of standards and samples for CAT activity.

CAT standards	Cf CAT (mg/mL)	Vi CAT (μL)	PBS (pH 7.4) (μL)	60 mM SPB/0.065 M H ₂ O ₂ (μL)	32 mM AMT (μL)
Blank	0	0	100	100	250
1	0.156	1	99		
2	0.313	2	98		
3	0.625	5	95		
4	1	7	93		
5	1.25	9	91		
6	2	14	86		
7	2.5	18	82		
8	3	21	79		
samples (50 μL)	-	-	-		

Table 13 | Preparation of standards for MDA calibration curve.

MDA standards	Cf MDA (mM)	Vi MDA Stock Solution (μL)	H ₂ O UP (μL)	Vi MDA standards (μL)	1.3% TBA/0.3% NAOH (μL)
Blank	0	0	200	0	75
1	2.5	0.5	190	10	
2	5	1			
3	10	2			
4	20	4			
5	30	6			
6	50	10			
7	80	16			
8	100	20			